AD-A159 497 FREE ELECTRON LASERS(U) CALIFORNIA UNIV SANTA BARBARA 1/1
QUANTUM INST W B COLSON ET AL AUG 85 TR-5
N00014-81-K-0809

UNCLASSIFIED F/G 20/5 NL

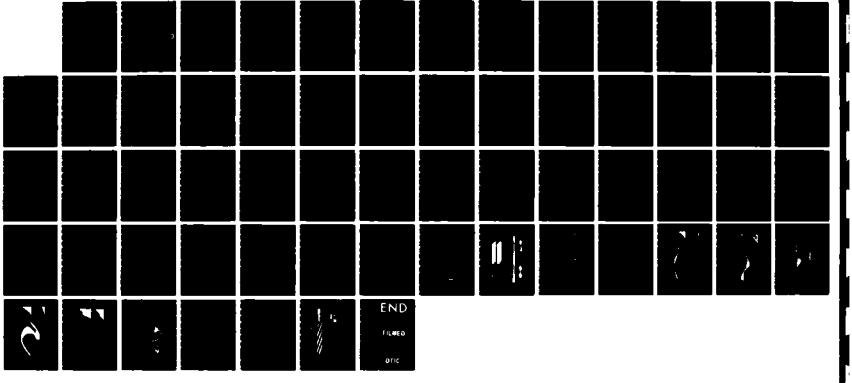

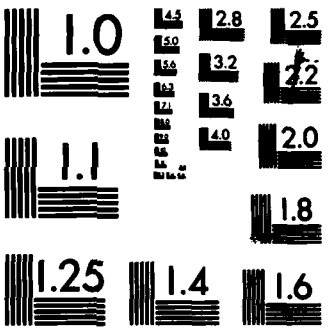

MICROCOPY RESOLUTION TEST CHART
NATIONAL BUREAU OF STANDARDS-1963-A

unclassified/ unlimited

SECURITY CLASSIFICATION OF THIS PAGE (When Data Entered)

(2)

REPORT DOCUMENTATION PAGE

READ INSTRUCTIONS BEFORE COMPLETING FORM

1. REPORT NUMBER: No. 5 TR-5	2. GOVT ACCESSION NO.: AD-A159497
3. RECIPIENT'S CATALOG NUMBER:	
4. TITLE (and Subtitle): Free Electron Lasers	5. TYPE OF REPORT & PERIOD COVERED: Final Technical Report 7/1/84 - 2/28/85
	6. PERFORMING ORG. REPORT NUMBER:
7. AUTHOR(s): W. B. Colson and A. M. Sessler	8. CONTRACT OR GRANT NUMBER(s): N00014-81-K-0809
9. PERFORMING ORGANIZATION NAME AND ADDRESS: University of California, Quantum Institute, Santa Barbara, CA 93106	10. PROGRAM ELEMENT, PROJECT, TASK AREA & WORK UNIT NUMBERS:
11. CONTROLLING OFFICE NAME AND ADDRESS: Office of Naval Research, 800 North Quincy Street, Arlington, VA 22217	12. REPORT DATE: August 1985
	13. NUMBER OF PAGES: 53
14. MONITORING AGENCY NAME & ADDRESS(if different from Controlling Office): Office of Naval Research, 1030 East Green Street, Pasadena, CA 91105	15. SECURITY CLASS. (of this report): unclassified/ unlimited
	15a. DECLASSIFICATION/ DOWNGRADING SCHEDULE:

16. DISTRIBUTION STATEMENT (of this Report)

Approved for public release; distribution unlimited.

17. DISTRIBUTION STATEMENT (of the abstract entered in Block 20, if different from Report)

Approved for public release; distribution unlimited.

18. SUPPLEMENTARY NOTES

Submitted to Annual Reviews of Nuclear and Particle Science.

19. KEY WORDS (Continue on reverse side if necessary and identify by block number)

review, free electron laser, theory, experiment

20. ABSTRACT (Continue on reverse side if necessary and identify by block number)

This paper reviews the experimental and theoretical developement of free electron lasers. There is a review of the types of accelerators driving FELs, the history of FELs, and the prospects for the future.

Keywords in abstract

DD FORM 1 JAN 73 1473 EDITION OF 1 NOV 65 IS OBSOLETE

S/N 0102-LF-014-6601

unclassified/ unlimited

SECURITY CLASSIFICATION OF THIS PAGE (When Data Entered)

OFFICE OF NAVAL RESEARCH

Contract N00014-81-K-0809

Final Technical Report No. 5

FREE ELECTRON LASERS

by

W. B. Colson and A. M. Sessler

ANNUAL REVIEW of NUCLEAR
and PARTICLE SCIENCE, Submitted

University of California
Quantum Institute
Santa Barbara, CA 93106

LBL-18905

FREE ELECTRON LASERS*

W. B. Colson
Berkeley Research Associates
P.O. Box 241
Berkeley, CA 94701

and

A. M. Sessler
Lawrence Berkeley Laboratory
University of California
Berkeley, CA 94720

January 1985

* This work was supported by the U. S. Air Force Office of Scientific Research Grant No. AFOSR-84-0079 (W.B.C.) and by the Office of Energy Research, U. S. DOE under Contract No. DE-AC03-76SF00098 (A.M.S.).

CONTENTS

1. Introduction

The free electron laser (FEL) uses a high quality relativistic beam of electrons passing through a periodic magnetic field to amplify a co-propagating optical wave (1-4). In an oscillator configuration, the light is stored between the mirrors of an open optical resonator as shown in Figure 1. In an amplifier configuration, the optical wave and an intense electron beam pass through the undulator field to achieve high gain. In either case, the electrons must overlap the optical mode for good coupling. Typically, the peak electron beam current varies from several amperes to many hundreds of amperes and the electron energy ranges from a few MeV to a few GeV. The electrons are the power source in an FEL, and provide from a megawatt to more than a gigawatt flowing through the resonator or amplifier system. The undulator resonantly couples the electrons to the transverse electrical field of the optical wave in vacuum.

The basic mechanism of the coherent energy exchange is the bunching of the electrons at optical wavelengths. Since the power source is large, even small coupling can result in a powerful laser. Energy extraction of 5% of the electron beam energy has already been demonstrated. The electron beam quality is crucial in maintaining the coupling over a significant interaction distance and of central importance to all FEL systems is the magnetic undulator. The peak undulator field strength is usually several kG and can be constructed from coil windings or permanent magnets. In the top part of Figure 2, the Halbach undulator design is shown for one period. The field can be achieved, to a good approximation, using permanent magnets made out of

rare earth compounds; a technique developed by K. Halbach (5), and now employed in most undulators. The undulator wavelength is in the range of a few centimeters and the undulator length extends for a few meters, so that there are several hundred periods for the interaction (6-8). The polarization of the undulator can be either linear or circular or a combination (9). The optical wave has the same polarization as the undulator driving it. This is an illustration of the FELs most important attribute ... the flexibility of its design characteristics.

The transverse undulations of electrons with energy γmc^2 generates spontaneous emission in a forward cone of angular width γ^{-1}. When the undulator fields are strong enough so that the amplitude of the cone's oscillation off axis is comparable to the cone's width, a detector on axis at infinity will begin to see several radiation harmonics (10). If the angular deviations of the cone are larger, then the spectrum becomes broadband like the synchrotron emission from a bending magnet. The total emission energy from a bending magnet and an FEL undulator are similar, but the FEL spectrum is confined to a relatively narrow bandwidth because the electron motion is periodic and the radiation cone stays on the undulator axis. The FEL gain bandwidth falls within the narrow spontaneous emission spectrum which is determined by the number of undulator period. The laser linewidth can be much narrower than the spontaneous linewidth as in an atomic laser; the narrow line and long coherence length is established by mode competition.

The laser frequencies driven by the FEL mechanism are much higher than the oscillation frequency of the electrons in the undulator. This is due to a large Lorentz contraction of the undulator wavelength and a

large relativistic Doppler shift of the emitted radiation in the forward direction. The relation between the undulator wavelength λ_u, the optical wavelength λ, and the electron beam energy is then $\lambda \approx \lambda_u/2\gamma^2$ and the mechanism can be described as stimulated Compton backscattering. It is the relativistic factor $2\gamma^2$ which allows the FEL to reach short wavelengths. Low energy beams (5 MeV) are being used to reach wavelengths longer than atomic lasers (500 microns) and high energy beams (1 GeV) are used for x-rays (500 Å) as shown in Table 1 (11-27). The FEL system is also continuously tunable merely by changing the electron energy of the electron source. Figure 3 shows some FEL system configurations which will be explained more fully in Part B.

Figure 2 illustrates the basic bunching mechanism used to obtain coherent radiation. The electrons leaving the accelerator are randomly positioned over many optical wavelengths. There are typically 10^7 electrons, or more, in each section of the electron beam one optical wavelength long. As the light and electrons interact at the beginning of the undulator some electrons gain energy and some lose energy. Those that gain energy move a little faster longitudinally and those that lose energy move a little slower; this creates one bunch in each optical wavelength.

FELs have been described in a number of articles in the general scientific press (28-37). In addition, there are a number of review articles on the subject (38,39,40) and there has been two special issues of IEEE J. Quantum Electronics on FELs containing many papers (41,42). Finally, there are six volumes of conference proceedings which contain

hundreds of papers, and which provide a good introduction to the FEL literature (43-48).

PART A: GENERALITIES

2. History

The historical development of FELs can be traced back to the microwave tubes of the 1940's shown at the top of Figure 4. The traveling wave tubes developed by H. Motz (49) were similar in structure to the FEL in that they used mildly relativistic electrons traveling through periodically undulating electric or magnetic fields inside a wave guide. The radiation wavelengths produced were in the centimeter range. A characteristic of all such devices was the closed structure used to store the radiation. The systems were tunable by changing the electron energy and using higher harmonics, and efficiencies of 60% were common. While the Motz tubes used the same configuration as the FEL, the operating mechanism was different. A tube that used the same mechanism as in an FEL was invented by Phillips (50), but J. M. J. Madey was unaware of the Phillips tube, although he did know of Motz's work. Shorter wavelengths could not be reached because electrons did not oscillate fast enough and the closed resonator could not be made small enough.

Atomic lasers were invented in the 1960's and made use of two new concepts (51): excited electrons in the bound states of atoms or molecules oscillated rapidly to produce optical radiation and this radiation was stored in open optical resonator.

J. M. J. Madey's conception of the FEL (1) came from a mixture of the attributes of microwave tubes and the atomic laser: the Motz undulator

and the optical resonator. The relativistic Lorentz contraction and the Doppler shift produced high frequencies from the slower oscillations of the electrons traveling near the speed of light. The FEL is tunable just as the early electron tubes but works at short wavelengths.

Independently, R. Palmer, P. Csonka, and K. Robinson were working on the coherent emission of radiation by relativistic electron beams (52).

3. Basic Concepts

A good theoretical approach to FELs is to solve the relativistic particle dynamics and couple the solutions to the optical wave equation. The more sophisticated analytical methods employed in the analysis of plasmas and lasers are appropriate, but generally not needed. The first classical theory was introduced by M. O. Scully, F. Hopf, et al (53).

The initial electron density has no structure on the scale of the FEL optical wavelength. Individual electrons are only influenced by the radiation field, the undulator magnetic field, and possibly the Coulomb fields of other electrons, if the density is large enough. For typical undulator fields and wavelengths, the radiation emitted spontaneously after just one pass is sufficient to define a classical wave. The Lorentz force equations for an electron are

$$\text{(a)}\ \frac{d}{dt}(\gamma\vec{\beta}) = -\frac{e}{mc}[\vec{E}_r + \vec{\beta}x(\vec{B}_u + \vec{B}_r)] \qquad (1)$$

$$\text{(b)}\ \frac{d\gamma}{dt} = -\frac{e}{mc}\vec{\beta}\cdot\vec{E}_r \quad ; \quad \text{(c)}\ \gamma^{-2} = 1 - \vec{\beta}\cdot\vec{\beta}\ ,$$

where $\vec{E}_r$ and $\vec{B}_r$ are the optical electric and magnetic fields, $\vec{B}_u$ is the undulator field, $e = |e|$ is the electron charge magnitude, c is the speed of light, m is the electron mass, $\vec{\beta}c$ is the electron velocity, and

γmc^2 is the electron energy. Only four of these five equations are needed to completely specify the problem. The undulator axis is taken along the z axis so that the transverse optical force with contributions contributions from both $\vec{E}_r$ and $\vec{B}_r$ is proportional to $|\vec{E}_r|\ (1 - \beta_z)$. For relativistic electrons $(1 - \beta_z) \approx 1/2\gamma^2$, so that the transverse optical force is small; the optical electric and magnetic forces combine to almost cancel when $\gamma >> 1$.

In order to couple energy out of the electron beam, the time average of $\vec{\beta} \cdot \vec{E}_r$ must be non-zero during the interaction time in the undulator. The role of the undulator is to rotate the transverse electron velocity as the field $\vec{E}_r$ passes over it. Note that in Eq. (1.a) the transverse electron motion is determined primarily by the undulator magnet since the transverse optical force is small. However, a randomly distributed electron beam will have $\langle \vec{\beta} \cdot \vec{E}_r \rangle = 0$ with no net energy transfer. But, an energy modulation alters the electron z velocities to cause bunching and coherent emission. While deflections off the mode axis are necessary for coupling, they cannot be too large, since the optical mode has a limited radial extent.

A suitable undulator field (6) around the mode axis is

$$B_x \approx - B \left\{ \left[1 + \frac{1}{8} k_u^2 \left(3x^2 + y^2\right)\right] \cos\left(k_u z\right) - \frac{1}{4} k_u^2 xy \sin\left(k_u z\right) \right\}$$

$$B_y \approx B \left\{ \left[1 + \frac{1}{8} k_u^2 \left(x^2 + 3y^2\right)\right] \sin\left(k_u z\right) - \frac{1}{4} k_u^2 xy \cos\left(k_u z\right) \right\} \qquad (2)$$

$$B_z \approx - B \left[1 + \frac{1}{8} k_u^2 \left(x^2 + y^2\right)\right] \left[x \sin\left(k_u z\right) + y \cos\left(k_u z\right)\right] \ ,$$

where B is the peak field strength and $\lambda_u = 2\pi/k$ is the undulator wavelength. The electron beams suitable for FELs must be sufficiently

aligned that the transverse excursions are small compared to λ_u. The average magnetic field strength increases off axis so that the electrons are focused toward the axis. When electrons are focused back toward the undulator axis, the transverse oscillations are called betatron oscillations. Typical transverse excursions are small enough that $k_u x$ and $k_u y$ are negligible.

With a small, high quality beam, the undulator field sampled by electrons is (B cos $(k_u z)$, B sin $(k_u z)$, 0) and the orbits, which are helical, are

$$\vec{\beta} = \left[(-K/\gamma) \cos (k_u z), (-K/\gamma) \sin (k_u z), \beta_z\right] \quad (3)$$

where $\beta_z \approx 1 - (1 + K^2)/2\gamma^2$ and $K = eB\lambda_u/2\pi mc^2$. Typically $K \approx 1$ and one sees that the transverse oscillations are small.

The optical field polarization which best couples to the above trajectory is given by the vector potential

$$\vec{A}(z,t) = \frac{E(t)}{k} [\sin (kz - \omega t + \phi(t)), \cos (kz - \omega t + \phi(t)), 0] , \quad (4)$$

where E(t) is the electric field magnitude, $\lambda = 2\pi c/\omega = 2\pi/k$ is the optical carrier wavelength, and $\phi(t)$ is the optical phase. No x or y dependence is included in $\vec{A}$, for now, since we assume the electrons remain well inside the optical mode waist. The optical electric field is $\vec{E}_r = -c^{-1}\partial\vec{A}/\partial t$. Inserting $\vec{E}_r$ and Eq. (3) into Eq. (1.b) we have

$$\frac{d\gamma}{dt} = \left(\frac{eKE}{\gamma mc}\right) \cos \left[(k_u + k) z - \omega t + \phi)\right] . \quad (5)$$

A particular useful form of Eq. (5) may be obtained in the case where the fractional energy change $\delta\gamma/\gamma \ll 1$. Define the electron phase $\zeta(t) = (k_u + k) z(t) - \omega t$, then eliminate $\gamma(t)$ from Eq. (5) to get

$$\frac{d^2\zeta}{d\tau^2} = \frac{d\nu}{d\tau} = |a| \cos(\zeta + \phi) \qquad (6)$$

where $|a| = 4\pi NeKLE/\gamma^2 mc^2$ is the dimensionless optical field strength, $\tau = ct/L$ is the dimensionless time, $L = N\lambda_u$ is the undulator length so that $0 \leq \tau \leq 1$, and $\nu = d\zeta/d\tau$ is the electron phase velocity. The electron dynamics have been put in the form of a pendulum equation (54).

The evolution of each electron entering the FEL undulator follows Eq. (6). Individual electrons are identified by their initial conditions $\zeta(0) = \zeta_0$ and $\nu(0) = \nu_0 = L[(k_u + k)\beta_z(0) - k]$. In weak fields $|a| << \pi$, and when $|a| >> \pi$, the fields are considered strong because the phases evolve significantly in the time $\tau \leq 1$. Experiments are usually designed so that the spread in electron velocities does not cause a spread in ν_0 greater than π. This can be adjusted by keeping the length L small enough, but a better beam quality allows a greater length L and much more gain.

The optical wave is governed by the wave equation driven by the current $\vec{J}_\perp$.

$$\left(\frac{\partial^2}{\partial z^2} - \frac{1}{c^2}\frac{\partial^2}{\partial t^2}\right)\vec{A}(z,t) = -\frac{4\pi}{c}\vec{J}_\perp(z,t) \quad , \qquad (7)$$

where the (x,y) dependence has been dropped (see Section 5). The transverse electron current is the sum of all particle currents

$$\vec{J} = -ec\sum_m \vec{\beta}_\perp\, \delta^{(3)}(\vec{x} - \vec{r}_m(t)) \qquad (8)$$

where $r_m(t)$ is the trajectory of the m^{th} electron and $\vec{\beta}_\perp = (\beta_x, \beta_y, 0)$. Even the spontaneous emission spectrum in an FEL has a long coherence

length so that the field E(t) and phase $\phi(t)$ can be taken to vary slowly over an optical period, ω^{-1}. Then, the terms containing second derivatives in Eq. (7) are negligible compared to terms with single derivatives and

$$\frac{d}{d\tau}(Ee^{i\phi}) = \frac{L}{c}\frac{d}{dt}(Ee^{i\phi}) = -\pi eKL\sum_m \frac{e^{-i\zeta}}{\gamma}\delta^{(3)}(\vec{x} - \vec{r}_m(t)) .$$

Then, the wave equation has the simple form

$$\frac{da}{d\tau} = -j\langle e^{-i\zeta}\rangle , \qquad (9)$$

where $a = |a|e^{i\phi}$, the dimensionless current density is $j = 8N(\pi eKL)^2\rho/\gamma^3 mc^2$, ρ is the electron particle density and the angular brackets represent a normalized average over the electrons. If electrons are bunched at the phase π, then the optical amplitude is driven with strength j during the time $0 < \tau < 1$; and there is gain. If the phase $\pi/2$ is over-populated, then the optical phase ϕ grows with little gain. Usually, it is a combination of $|a|$ and ϕ that are driven because the electron bunching is not perfect.

Figure 5 shows the phase space evolution of a periodic section of the electron beam in the (ζ,ν) coordinates. The separatrix path shown is given by $\nu_s^2 = 2|a|(1-\sin(\zeta_s+\phi))$; the peak-to-peak height is $4|a|^{1/2}$ and the horizontal position is determined by ϕ. The "fluid" of electrons starts equally populating all phases and at the phase velocity $\nu_0 = 2.6$ for maximum gain. As the electron fluid evolves in the Figure it becomes darker to black at $\tau = 1$. The final bunching is near the phase π and the gain and optical phase shift evolution are shown at the right. The initial optical field is weak $a(0) = a_0 = 1$, and the final gain determined numerically is $G \equiv [|a(1)|^2 - a^2(0)]/a^2(0) = 0.135j$.

While we have made a few assumptions, the "pendulum" and wave equations, Eq. (6) and Eq. (9), form a simple, powerful description of the FEL (54). They are valid for both weak ($|a| << \pi$) and strong ($|a| >> \pi$) optical fields in either high ($j >> 1$) or low ($j << 1$) gain conditions. It is generally important that both the optical field amplitude and phase are included in the description.

When the optical fields are weak, Eq. (6) and Eq. (9) can be easily linearized in $a(\tau)$:

$$\dot{a} = ij < e^{-i(\zeta_0 + \nu_0\tau)} \xi_1 > \quad ; \quad \ddot{\zeta}_1 = |a| \cos(\zeta_0 + \nu_0\tau + \phi), \tag{10}$$

where $(\cdot) = d(\,)/d\tau$, $\zeta = \zeta_0 + \nu_0\tau + \zeta_1$, and ζ_1 is ζ to lowest order in $|a|$. For a uniform beam distribution

$$< > = \int_0^{2\pi} d\zeta_0 \,(\,)/2\pi \ ,$$

the electron coordinates can be removed from Eq. (10) and the optical field is determined by the roots to the cubic equation

$$\alpha_r^3 - i\nu_0 \alpha_r^2 - (\tfrac{i}{2})\, j = 0 \ , \tag{11}$$

with the field of the form $a = a_0 e^{-i\nu_0\tau} \sum_{r=1}^{3} e^{\alpha_r\tau}$. If $|\nu_0| >> \pi$ so that the FEL is far off-resonance, the driving term j is negligible and the trivial uninteresting solution $a \simeq a_0$ is obtained; i.e. no gain. If the current density j is large, so that ν_0 is negligible the important real root is $\alpha_r = (j/2)^{1/3}\,(\sqrt{3}/2)$ giving exponential growth. The complex field is then described by $a(\tau) = (a_0/3)\exp[(j/2)^{1/3}\,(\sqrt{3} + i)\,\tau/2)]$, and the gain is exponential after an initial bunching time.

Figure 6 shows the phase space evolution in the high gain case where $j = 100$. The electrons are started at $\nu_0 = 0$ to show how gain is achieved

on-resonance. Bunching occurs at the phase $\pi/2$ but in the high gain case, a significant optical phase shift changes the position of the separatrix so that, relative to the optical wave, bunching is at phase π. The resulting exponential growth and phase evolution are shown on the right. The exponential gain only occurs after bunching is established.

In the low gain case, both ν_0 and j are important in Eq. (11). The gain is no longer exponential and all three roots are needed to find the final gain at $\tau = 1$, which is given by:

$$G(\nu_0) = j \frac{[2-2\cos\nu_0 - \nu_0 \sin\nu_0]}{\nu_0^3} = -\frac{j}{2}\frac{d}{d\nu_0}\left(\frac{\sin(\nu_0/2)}{(\nu_0/2)}\right)^2 . \qquad (12)$$

The gain is antisymmetric in ν_0 and peaks at $G = 0.135j$ with $\nu_0 = 2.6$. Figure 7 shows the plot of $G(\nu_0)$ above the accompanying optical phase shift $\phi(\nu_0) = j\,[2\sin\nu_0 - \nu_0(1+\cos\nu_0)]/\nu_0^3$. Note that the gain spectrum can be written as the derivative of the spontaneous emission spectrum $[\sin(\nu_0/2)/(\nu_0/2)]^2$. This remains true for a large class of undulator designs and is known as the Madey theorem (55). The theorem states that when an undulator design produces a spectrum $s(\nu_0)$ the gain is proportional to the slope of the spectrum $ds(\nu_0)/d\nu_0$. A second theorem relates the "second moment of the mean electron energy loss evaluated to first order in the optical field strength," $\langle[\delta\gamma^{(1)}]^2\rangle$, to the "mean energy loss evaluated to second order in the optical field strength," $\langle\delta\gamma^{(2)}\rangle$,:

$$\langle \delta\gamma^{(2)} \rangle = \frac{1}{2}\,\frac{\partial}{\partial\gamma}\langle[\delta\gamma^{(1)}]^2\rangle \ .$$

In the FEL oscillator, gain over many passes leads to strong fields. The spontaneous fields either experience exponential growth or the

repeated gain of Eq. (12). In stronger fields where $|a| \gtrsim \pi$, the gain process changes and begins to depend on $|a|$. Electron phases now evolve too far in phase space and bunching is difficult to maintain. Figure 8 shows electrons in a strong field $a_0 \equiv |a(0)| = 8$. The separatrix is now large and electrons are trapped in the closed orbit region of phase space. Those near the harmonic circular paths oscillate around the phase $\pi/2$ at a frequency $|a|^{1/2}$; these oscillations are called synchrotron oscillations. There is a decrease in gain; i.e. saturation. When the gain is reduced to equal the FEL system losses, steady-state operation is established.

A method used to extend the saturation limit of FELs was proposed by Kroll, Morton, and Rosenbluth and is called the tapered undulator (56). As electrons lose energy to the optical wave, the undulator properties can be modified to accommodate the new electron energy. As γ decreases either the undulator wavelength, λ_u, or field strength, B, can be decreased to maintain resonance. A simple case is where both B and λ_u change along the undulator so that K is constant. When such a taper is included, the pendulum equation acquires an accelerating term, $\delta = L^2 dk_u(z)/dz$,

$$\ddot{\zeta} = \delta + |a| \cos(\zeta + \phi) \quad . \tag{13}$$

In the absence of the field $|a|$ electrons appear to be "accelerated" to higher phase velocities. In strong fields, about half the electron phases are trapped near the phase π which drives the optical amplitude and gain. Figure 9 shows the final position of electrons in phase space after trapping has occurred in strong fields $a_0 \approx 40$ and with tapering such that $\delta = 6\pi$. The untrapped electrons are seen at the top of the

phase space picture spread over the phase axis randomly. The gain is higher than would be possible at this field strength without tapering. The tapered undulator is a good example of the design flexibility of FELs. The undulator structure (length, polarization, wavelength profile, field profile B(z), etc.) are all features that can be modified to enhance performance for a particular FEL application.

An example proposed by Vinokurov and Shrinsky is the klystron FEL (sometimes called a transverse optical klystron FEL, or TOK) where the undulator is split into two sections separated by a drift or dispersive section (57). The purpose is to achieve higher gain for a given interaction length L. The dispersive section acts like the bending magnet of an electron energy analyzer. Small variations in the electron phase velocity ν caused by the first undulator section are translated into phase changes $\Delta\zeta = D\nu$ at the end of the dispersive magnet and the parameter D measures the strength of the dispersive field. The theoretical description of the field and the electrons uses Eq. (6) and Eq. (9) with $\Delta\zeta = D\nu$ applied to each electron at $\tau = 1/2$. This results in a higher degree of bunching, and therefore greater gain than given by Eq. (12).

When the undulator is designed to have linear polarization, only the definitions of variables in Eq. (6) and Eq. (9) change while the form of the equations remains the same. The modifications are $a \rightarrow a\,[J_0(\xi) - J_1(\xi)]$, $j \rightarrow j\,[J_0(\xi) - J_1(\xi)]^2$, where $\xi = K^2/2(1 + K^2)$ and B becomes the rms undulator field strength.

4. Transverse Effects

The one-dimensional analysis, which we have employed up to this point, leaves out all transverse effects except the simple periodic undulator motion.

First we shall discuss electron beam transverse effects. A helical undulator provides focusing of the electrons in both transverse planes. Sometimes, a longitudinal, solenoidal field is employed so as to give even more focusing. For some devices the cyclotron resonance in this field coincides, or almost coincides, with the FEL resonance and makes the interpretation of these experiments more complicated (12). On the other hand, this juxtaposition appears to enhance the gain, but is limited to long wavelength applications because of the upper limit on attainable solenoidal field strengths.

For planar undulators there is only "natural" focusing in the plane perpendicular to the sinusoidal motion and the betatron wave number is $k_{By} = eB/\sqrt{2}\, mc\gamma$ in the non-wiggle plane, where B is the peak field. The resonance condition is maintained as a particle undergoes betatron oscillations. In the wiggle plane, generally some focusing is required (50,58,59). Quadrupoles, although they give focusing, seriously degrade FEL performance. A planar undulator field is

$$\vec{B} = -B \cosh(k_u y)\cos(k_u z)\vec{y} + B \sinh(k_u y) \sin(k_u z)\vec{z} \quad ,$$

so that the motion is

$$x' \equiv \frac{dx}{dz} = \frac{B}{\gamma}\left(1 + \frac{k_w^2 y^2}{2} + \ldots\right) \sin(k_w z) \quad ,$$

and hence increases as y increases. This increase with y just balances the decrease of $y' \equiv dy/dz$ when y increases and causes β_z to be constant. E. T. Scharlemann (60) has shown how shaping the undulator pole faces with a slight parabolic curvature provides horizontal focusing while maintaining β_z a constant of the motion. The curvature causes the field to increase off axis and provides focusing in both x and y. If the pole face is given by $y(x) = Y_0 (1 - k_u^2 x^2/4)$, then the focusing will be the same in x and y and the electron beam cross section will be round.

It is necessary, in any real FEL, to avoid resonances between the various frequencies to which the particles are subject. For example, one must avoid a resonance between betatron oscillations and integral multiples of λ_u. Also, one must avoid the usual coupling resonances between the betatron oscillations in x and y. There is another kind of resonance which must also be avoided and this is a synchro-betatron resonance between the "synchrotron motion" of trapped electrons and transverse betatron motion (61,62).

We turn, now, to transverse effects of the electromagnetic wave. The simplest effect is the excitation of cavity modes in an oscillator. Figure 10 shows this phenomenon in a computer simulation of the original Stanford experiment where the electron beam has been moved off-axis to excite a combination of higher order modes.

The Rayleigh range is a measure of the effect of diffraction. For a light beam of radius w, the Rayleigh range $z_r = \pi w^2/\lambda$ is the propagation distance over which the optical wavefront doubles its area. In a proper FEL design one wants good overlap between the electron beam and the light beam over the whole interaction length so that z_r should be comparable

to L. However, if the FEL has sufficiently high gain it can provide "guiding" to the light and keep it within the electron beam for many Rayleigh lengths as in an optical fiber (63,64). This is seen, dramatically, in Figure 11.

An FEL provides an effective index of refraction, n, by changing the optical phase along the interaction length.

$$\mathrm{Re}(n) - 1 \equiv \frac{1}{k}\ \frac{d\phi}{dz} = \frac{j}{k|a|L} \langle \sin(\zeta + \phi) \rangle \ ,$$

and

$$\mathrm{Im}(n) - 1 \equiv \frac{1}{k|a|}\ \frac{d|a|}{dz} = \frac{-j}{|a|Lk} \langle \cos(\zeta + \phi) \rangle \ .$$

For an optical fiber, guiding occurs if $\mathrm{Re}(V^2) + \frac{1}{2}\,\mathrm{Im}(V^2) > 1$, where the (complex) fiber parameter, V, is given by $V^2 = (n^2 - 1)b^2k^2$, where b is the electron beam radius. Thus one can readily determine when guiding takes place, provided one can evaluate the averages over particles of $\sin(\zeta + \phi)$ and $\cos(\zeta + \phi)$. When there is gain, we know that the averages of sin and cos are non-zero.

In the exponential growth regime one can evaluate the averages analytically (63,64,65). One simply augments the wave equation, Eq. (7), with $\nabla_\perp^2$ and then approximates this transverse derivative with

$$\nabla_\perp^2 E \approx -\frac{2kE}{z_r} \ .$$

The result is that Eq. (11) becomes, for $\nu_0 = 0$,

$$\alpha_r^3 + i\,\alpha_r^2\,(L/z_r) - (\tfrac{i}{2})\,j = 0 \ ,$$

where the length of the undulator is L. Thus the effect of diffraction and optical guiding are included in a one-dimensional theory. Extension

to a warm beam and to $\nu_0 \neq 0$ can be found in the quoted literature (63,64,65).

5. Longitudinal Effects

The simple pendulum and wave equations, Eq. (6) and (9), are valid for a single complex field $a = |a|e^{i\phi}$ with only a single frequency, the carrier frequency ω. A realistic FEL oscillator, or amplifier, produces a spectrum of frequencies surrounding the carrier wave. Usually, the coherence length extends over several optical wavelengths so that the slowly varying amplitude and phase approximation remain valid. To generalize the optical field representation to many modes, the single complex field $a(\tau)$ becomes $a(k,\tau)$ or $a(z,\tau)$.

Driving the carrier phase ϕ in the center of the optical wavefront will focus the light along the electron beam path. Even in low gain diffraction couples the transverse and longitudinal waves. The phase profile $\phi(z)$ in a low gain oscillator is determined by the resonator mirrors and their Rayleigh length z_r. This causes a shift in frequency and a shift in the gain spectrum in an oscillator (66).

Often, the lack of distinct electron energy levels leads to questions about the ultimate coherence capabilities of FELs. In both the FEL and atomic laser, a long coherence length and narrow frequency spectrum is determined by mode competition, not by energy levels. In the low gain case, the weak field gain per pass in each mode is given by Eq. (12). The number of modes within the gain bandwidth is about γ^2 (typically $\gamma^2 >> 1$). Figure 12 shows the evolution of 100 optical wavelengths, around resonance. The spontaneous emission above resonance experiences

gain every pass while other wavelength receive less gain or absorption. The vertical scale follows the photon number $n(\lambda)$ over six order of magnitude in one-hundred passes. The spectrum clearly narrows as mode competition continues. The photon number evolves as exp $[G(\lambda)\ n_p]$ where n_p is the pass number in the low gain oscillator where modes are uncoupled.

Short pulse effects (67) in FELs can also be described by generalizing the field to a(k). An essential concept is "slippage"; this is the distance that light travels over the electron beam while the electrons travel through the undulator. It is given by $L(1 - \beta_z) \approx N\lambda$ using the FEL resonance condition. The ratio of the slippage distance $N\lambda$ to the electron pulse length σ_z determines whether or not short effects are important. If $N\lambda << \sigma_z$, then the pulse is considered long, and each part of the pulse experiences gain proportional to the local density. If $N\lambda >> \sigma_z$, then the FEL has short pulses and the modal structure of the pulse is comparable to the gain bandwidth, $\approx N^{-1}$.

Since electrons bunch when they reach the trailing edge of the optical pulse, the optical pulse receives more gain on its trailing edge than on its leading edge and behaves as if it is traveling slower than the speed of light, c; this effect is called "lethargy" (68) and must be considered in the oscillator FEL, where the resonator mirror spacing and the electron pulse repetition time must be synchronized (69,70). The range of mirror positions to achieve synchronism is astonishing small: only a four micron range was observed in the Stanford experiment. The amount of synchronism within the working range is important in determining the laser linewidth and power.

Other longitudinal effects involve long pulses in the FEL. One is the "trapped particle" instability analyzed by Kroll and Rosenbluth (71). The synchrotron frequency $|a|^{1/2}$ can mix with the carrier wave and produce sideband gain in the FEL. Figure 13 shows the growth of sideband structure in $|a(z)|$ and $\phi(z)$. A window section of a long pulse is four slippage distances long ($-2 < z/N\lambda < 2$). The field $|a(z)|$ is plotted at the top left with bright regions indicating an intense field and dark regions indicating a low field region. The pass number is plotted along the vertical axis. The "trapped particle" instability starts a modulation in the field magnitude $a(z)$ and the phase $\phi(z)$ with a period equal to the slippage distance. The final spectrum, the fourier transform of $a(z)$ is shown with its sideband on the bottom right; above is the weak field gain spectrum for reference. The final electron energy spectrum is shown above the gain spectrum. The power and net gain evolution are plotted on the upper right as a function of pass number n. The trapped particle instability is expected in nearly all FELs which saturate because of strong fields.

In a linearly polarized undulator, the electron z motion is more complex than in the helical case because there is a periodic oscillation of the electron z velocity even when injected perfectly. The oscillation in z, Δz, is given by $k\Delta z \approx -\xi \sin(2k_u ct)$ where $\xi = K^2/2(1+K^2)$. Since typically $K \approx 1$, the oscillations are a sizeable fraction of the optical carrier wavelength and lead to spontaneous emission and gain in higher optical harmonics (72). To generalize Eq. (6) and Eq. (9) for a harmonic hk, make the replacements: $\zeta \rightarrow h\zeta$, $\nu \rightarrow h\nu$, $a \rightarrow ah$,

$[J_{\frac{h-1}{2}}(h\xi) - J_{\frac{h-1}{2}}(h\xi)]$, and $j \to j\, h\, [J_{\frac{h-1}{2}}(h\xi) - J_{\frac{h+1}{2}}(h\xi)]^2$.

The form of the equations stays the same, only the couplings are modified. Note that there is gain only in the odd harmonics h = 1, 3, 5, ... If the undulator field is large enough so that $K \gtrsim 2$, then the coupling to higher harmonics is very strong. Several of the FEL-experiments to date have observed coherent emission into higher harmonics, and it should prove to be a useful technique for reaching shorter wavelength in an FEL.

PART B: FEL SYSTEMS

FELs can be made in a variety of configurations as is depicted schematically in Figure 3. In Part B, we describe in more detail a particular linac oscillator, a linac amplifier and a storage ring oscillator experiments. FEL systems are rapidly evolving and in the future can be expected to be quite different from those described here.

In Table 1 we have presented a compendium of those FELs which have operated. Many more FEL devices are under construction and, as one can see from the dates in Table 1, these devices are being brought into operation at an ever-increasing rate. In Table 2 (73-87) we present a representative list of FEL accelerators.

Of great importance to FELs are electron beams of high quality. Two figures of merit of quality, for a given current, are energy spread and brightness. The brightness is defined by $\mathcal{B} = \pi^2/\gamma^2\, \delta^4 V$, and becomes a measure of "goodness," where I is the current enclosed within the transverse 4-volume ($\delta^4 V = \delta x \delta x' \delta y \delta y'$). For uniform phase space density, the brightness can be approximated by $\mathcal{B} \simeq 2I/\gamma^2 \delta x \delta x' \delta y \delta y'$. The quality of a

beam depends upon the parameters of the accelerator, the type of accelerator and, of course, with what care it is aligned, etc. In Table 2 we present brightness and energy spread for a number of accelerators. As one can deduce, the expected performance of FELs far exceeds present achievements.

The development of FELs has been the result of both theoretical advances, which we have emphasized in this article, and of experimental advances. In fact, without the latter, we would only have an empty theoretical structure. The experimentalists who have been instrumental in the development of FELs are many in number and, of course, are cited in the references, but special note should be taken of the work of C. A. Brau, D. Prosnitz, D. A. G. Deacon, J. Eckstein, L. Elias, E. Shaw, S. Skrinski, B. Kincaid, C. Pellegrini, J. M. Ortega, M. W. Poole, A. Renieri, P. Elleaume, T. Smith, A. Gover, J. A. Edighoffer, J. M. Slater and G. Dattoli.

6. The Linac Oscillator

The experiment of the TRW Group (15) serves to illustrate the linac oscillator. The superconducting accelerator at Stanford has a bunch length 4.3 ps, peak current of 0.5–2.5 A, and at 66 MeV an energy spread of 0.03% and a beam emittance of $1.5\pi \times 10^{-5}$ m-rad. The optical cavity had mirrors 12.68 m apart with 7.5 m radius of curvature. At the optical wavelength of 1.57 μm, the reflectivity was 99.84%. The undulator consisted of pairs of linear arrays of Sm CO_5 permanent magnets with wavelength $\lambda_\mu = 3.6$ cm and a peak field of 2.9 kG.

The experiment was designed to study the effect of tapering. Furthermore they devised an optical klystron so the multicomponent undulator had

the following structure. First, there was a prebuncher section of 15 periods, then a magnetic dispersion section of two periods and total length 58.6 cm. Then 90 periods followed which could be tapered and, finally, 15 periods of constant undulator. The tapered part was varied to be a 0%, 1% and 2% taper in energy. Beam diagnostics consisted of 14 insertable flourescent screens so as to be sure the beam was steered properly and the mirrors were aligned using a green light laser.

With a 1% taper, the FEL had an average output laser power of 4 W and the peak power was 1.2 MW. Since the mirror transmission was 0.13% on each end of the cavity, the intracavity optical power was 11 GW/cm^2. The repetition rate was 10 Hz and the macropulse length 5 ms with the micropulse of 4 ps. The radiation fundamental was at 1.57 μm and the laser bandwidth was 1.3%.

Above threshold for the laser, the power increased by a factor of 10^{10} over that of the spontaneous radiation! The FEL took 305 passages at a gain of 7% per pass to get to 10% of the saturated level. The experimenters also observed coherent radiation at the second and third harmonic of 1.6 μm.

A study was made of the effect of tapering the undulator. For an untapered case the electron transfer of energy, efficiency, should be (1/2N). The efficiency was measured to be 0.4% which compares well with the expected value. With a 1% taper the electrons clearly divided into two groups: trapped and untrapped. Most, 60%, of the electrons were trapped and decelerated 1% to 1.8% while the untrapped electrons were unchanged in energy. Thus the beneficial effect of tapering was demonstrated.

7. The Linac Amplifier

The experiment of the LBL/LLNL is representative of this class of FELs (88,18). The FEL was run as a single-pass amplifier in the microwave range at 34.6 GHz. The input signal was supplied by a magnetron of peak power 60 kW and a pulse length of 500 nsec.

Use was made of the LLNL Experimental Test Accelerator (ETA) (73) to provide a 6 kA, 3.3 MeV beam with a normalized emittance of 1.5 π rad-cm. An emittance filter was used to reduce the beam current to approximately 500 A with a normalized edge emittance of 0.47 π rad-cm. The highly chromatic transport of the ETA beamline and matching quadrupoles results in a 15 ns, nearly monoenergetic beam delivered to the interaction region.

The undulator magnet was three meters long, and the undulator period was 9.8 cm. The longitudinal variation of the undulator field provided strong vertical focusing. Horizontally focusing quadrupole magnets, surrounding the undulator, provided horizontal focusing while only slightly reducing the vertical focusing and negligibly effecting the FEL resonance condition.

The interaction waveguide was a rectangular, oversized waveguide immersed in the undulator. The inside dimensions of the waveguide were 9.83 cm wide by 2.91 cm high. The electric field was horizontal and coupled to the TE_{01} waveguide mode which was excited by the input microwave signal.

The signal gain in the amplified spontaneous emission mode (no microwave input signal) was measured and it was found that the microwave signal grew at a rate of 13.4 dB/meter for a beam current of 450 A. Extrapolating this growth back to the origin, the effective input noise was 0.35 W.

The amplifier gain was studied both as a function of undulator magnetic field intensity and as a function of undulator length. The peak output power of 80 MW was achieved for both the 2 m and 3 m long undulator. The amplifier went into saturation at 2.2 meters; beyond this point, the amplified output power first decreased and then near 3 m started to increase again. The gain as a function of undulator length showed an exponential gain of approximately 15.6 dB/m up to saturation. This was in close agreement with the small signal gain measurement. The gain curves for the 1 m and 2 m undulators are relatively symmetric about the peak while the gain curve for the 3 m long wiggler shows a marked asymmetry with a plateau on the long wavelength side of the curve. This asymmetry at saturation is also shown in the numerical simulations.

Study of excitation of other than the TE_{01} mode, and study of the effect of varying the undulator parameters (so as to avoid saturation at 80 MW) are to be undertaken in the near future. What has been shown, so far, is that an FEL can be operated in the high gain regime (Gain $\gtrsim$ 2500).

8. Storage Rings

The first, and so far the only, operation of a storage ring FEL oscillator was achieved by the Orsay-Stanford collaboration using the Orsay ring ACO (16,89). This laser operated in the visible, at 6,500 Å, and produced 75 μw average power or 60 mW output peak power. The intracavity peak optical power was 2 kW.

The ACO storage ring has a circumference of 22 m and was operated between 160 MeV and 166 MeV. Two bunches were employed, with the average

current between 16 mA and 100 mA. The rms bunch length was (in time units) 0.5 ns to 1 ns and the energy spread (rms) 0.9×10^{-3} to 1.3×10^{-3}. Because of the strong radiation damping, the transverse size (rms) was 0.3 mm to 0.5 mm, corresponding to an angular spread of 0.1 mrad to 0.2 mrad.

The optical cavity was 5.5 m long so the round trip time resonated with the 11 m between electron bunches. The mirror radius was 3 m, the Rayleigh range 1 m. Although the mirror transmission was only 3×10^{-5}, the round-trip cavity loss was 7×10^{-4} due, primarily, to absorption in the mirror dielectric. In fact, there was mirror degradation due to the radiation harmonics of the undulator which forced the experimentalists to operate ACO at a reduced energy (originally they had expected to be at 240 MeV) and to operate the undulator at reduced magnetic field ($K = 1.1$ to 1.2), both effects tending, of course, to reduce the flux at higher harmonics.

The permanent magnet undulator had 17 periods with a period of 7.8 cm, and a total length of 1.33 m. It was operated as an optical klystron, in order to increase the gain per pass. This increased the gain by about a factor of 2 to 7 so as to reach 2×10^{-4} per pass. Lasing with such low gain required careful alignment of the electron beam on to the axis of the optical cavity, high quality mirrors, as well as precise synchronism between the light pulse reflections and the electron bunch revolution frequency. The detuning curve gave only a 1.6 μm full width at half maximum near laser threshold.

The laser time pulse structure was a series of pulses and showed the electron rf synchrotron frequency, (13 kHz), and the 27.2 MHz bunch frequency. The time sequence of pulses is understood as a consequence of theoretical study (90). In frequency space the laser had three lines (near 6500 Å) with the dominant one at 6476 Å. All the lines, corresponding to maximum gains in the klystron FEL were in the TEM_{00} mode. The width of the lines was 2 Å - 4 Å. Tunability was over 150 Å and limited by mirror reflectivity.

The storage ring FEL is the only configuration mentioned wnere the FEL feeds back on the electron source. On each pass the working FEL "heats" the electron beam by introducing an energy spread. Synchrotron radiation P_{syn} from the bending magnets in the ring damp the excitations. The laser power at saturation is determined by thermodynamic equilibrium which results in weak fields; this is the Renieri limit (91), $P_{laser} = P_{syn}/2N$. The efficiency of the FEL was only 2.4×10^{-5} which is 0.4 of the prediction of Renieri for this case.

9. Extensions

We have seen that FELs can be expected to be efficient, powerful, reliable, tunable sources of radiation in a wide range of wavelengths. In fact, FELs have already been made to operate from the microwave range down to the visible range. It is reasonable to expect that soon we shall have FELs readily available, for many different applications, from microwave wavelengths to soft X-ray wavelengths. When augmented with atomic and molecular lasers and conventional radio tube sources, we can expect to have coherent radiation sources throughout the radiation spectrum (presently, one can see one's way to 300 Å).

Why then should one develop even more devices? Clearly, because they can be designed for special purposes, have special properties, be less expensive, more efficient, etc. The development of FELs is far from completed and really only starting; there are a number of extensions of FELs which appear to be possible. Here, we shall mention a few of them and refer the interested reader to the appropriate literature.

In the microwave range it is possible to apply a longitudinal magnetic field of sufficient strength that the cyclotron frequency resonates with the radiation frequency. Thus one can arrange a device where there is coincidence between the FEL resonance and the cyclotron resonance as described in Section 4 (12,92,93).

It is possible to replace the undulator with an electromagnetic field. The attainable magnetic field of an rf-wave is less than that of a static or pulsed magnetic field, but the wavelength of the "undulator" can be made less than that of a conventional undulator. Thus, one can get to short wavelengths with a low-energy electron beam. The use of an rf wave as an undulator has already been demonstrated (94) and demonstration has been made of an electromagnetic wave undulator FEL by an NRL group (95). This group had the electron beam produce 500 MW of 12.5 GHz radiation through a backward wave oscillator mechanism, and then used this radiation as an undulator for FEL action. In this manner they produced 200 GHz radiation with peak power, not yet optimized, 0.35 MW. The Santa Barbara group (96) plans to employ the same idea, but employ the FEL mechanism to generate the rf field of an "undulator" in a "two-stage FEL".

We have concentrated upon so-called "Compton regime FELs" where there is a strong interaction between the electrons and the optical wave, but where the interaction between electrons is small. In the opposite case, where the electrons interact strongly through Coulomb forces, so that a density fluctuation, or plasmon, description of the electron beam is more appropriate, the FEL is said to be in the "Raman regime". An understanding of the collective regime, the Raman regime, is more difficult than that of the Compton regime, but offers distinctive features. Experiments (12) have demonstrated 6% conversion efficiency, and large power emission (75 MW) in this regime. One can expect more development of these devices in future years (97).

An interesting extension of the FEL is to operation in a dielectric media (98,99). Gas loading, for this is the proposed manner to realize the dielectric media, changes the phase-matching condition and so allows a wider parameter space than the vacuum FEL. In fact, this extension can be non-trivial and would appear to allow operation, for example, at smaller undulator magnetic fields than in the conventional FEL. The resonance condition, for relativistic electrons is $n - 1 + \lambda/\lambda_u = (1 + K^2)/2\gamma^2$, for a medium having an index of refraction n. Note that the $(n - 1)$ term can easily be comparable to the usual $(1/2\gamma^2)$ FEL term. One can think of this device as being a suitable combination of the Cerenkov effect and the FEL resonance.

Another interesting extension of a conventional FEL is to have an undulator in an isochronous storage ring (100,101) in which particles with different energies take exactly the same time to go around the ring. Thus bunching at optical wavelengths is preserved around the

ring. Most rings do not have this property and thus the electron bunch on entering the undulator is essentially a "new bunch" with random phases. Rings can be made isochronous, to some degree, so that the bunching of an FEL can be preserved. Clearly this is advantageous, and it can be done so as to preserve far-infra-red wavelength bunching as has been shown on BESSY (102). An FEL using this concept has not yet been made; it is doubtful that the technique can be extended into the visible, but for the infra- red it could make a very interesting device.

Finally, it should be emphasized that "pushing" FELs to shorter and shorter wavelengths, as has been spearheaded by J. M. J. Madey and C. Pellegrini, may require no "new inventions," but, nevertheless, be difficult and a significant extension. This subject, as one might expect, has received considerable effort (85,87,103,104). Suffice it to say, here, that it appears possible to construct an FEL oscillator down to about 500 Å, and a single-pass FEL growing from noise to about 300 Å. Just what the limits are remains to be seen, but the possibility of extending the Orsay achievement by an order-of-magnitude appears to be possible.

Acknowledgements

We are grateful for support from the U. S. Air Force Office of Scientific Research Grant No. AFOSR-84-0079 (W.B.C.) and from the Office of Energy Research, U. S. DOE under contract DE-AC03-76SF 00098 (A.M.S.).

Literature Cited:

1. Madey, J. M. J., J. Appl. Phys., 42, 1906 (1971).
2. Madey, J. M. J., Stimulated emission of radiation in periodically deflected electron beam, U. S. Patent 3,822,410 (1974).
3. Elias, L. R., Fairbank, W. M., Madey, J. M. J., Schwettman, H. A., and Smith, T. I., Phys. Rev. Lett., 36, 717, (1976).
4. Deacon, D. A. G., et al, Phys. Rev. Lett., 38, 892, (1977).
5. Halbach, K., see Ref. 47, p. C1-211.
6. Blewett, J. P. and Chasman, R., J. Appl. Phys., 48, 2692, (1977).
7. Elias, L. R. and Madey, J. M. J., Rev. Sci. Inst., 50, 1339, (1979).
8. Diament, P. Phys. Rev. Lett., A23, 2537 (1981).
9. Kim, K-J., Nucl. Instr. and Method., 219, 425 (1984).
10. Colson, W. B., "Free electron laser theory," Ph.D. dissertation, Stanford University, (1977).
11. Deacon, D. A. G., et al, Phys. Rev. Lett., 38, 892 (1977).
12. Gold, S. M., et al, see Ref. 48, p. 350.
13. Newnam, B. E., et al, see Ref. 11, p. 118.
14. Grossman, W. M., et al, see Ref. 11, p. 52.
15. Edighoffer, J. A., et al, Phys. Rev. Lett., 52, 344 (1984).
16. Billardon, M., et al, Phys. Rev. Lett., 51, 1652, (1983).
17. Pasour, J. A. Lucey, R. F. and Kapetanakos, C. A., Phys. Rev. Lett., 53, 1728 (1984).
18. Orzechowski, T. J., et al, submitted for publication in Phys. Rev. Lett. (1985).
19. Fajans, J., Bekefi, G., Yin, Y. Z., Lax, B., Phys. Rev. Lett. 53, 246 (1984).

20. Robinson, A. L., reported in Science 226, 154 (1984).

21. Dolezal, F., Harvey, R., Palmer, A., paper presented at the Ninth Int. Conf. on Infrared and Millimeter Waves, Osaka (Oct 1984).

22. Barbini, R., et al, see Ref. 47, p. C1-1.

23. McDermott, B. D., et al, Phys. Rev. Lett., 41, 1368 (1978).

24. Omatuni, T. S., Petrosian, M. L., Petrosian, B. V., Shahbazian, N. T., Oganesian, K. B., Erevan EPI-727 (42)-84 (unpublished 1984).

25. Marshall, T., et al, Appl. Phys. Lett., 31, 320 (1977).

26. Granatstein, V., et al, Appl. Phys. Lett., 30, 384 (1977).

27. Artamonov, et al, Nucl. Instr. and Methods, 177, 247 (1980); Kornyuikhin, G. A., et al, Institute of Nuclear Physics, Novosibirsk, Internal Report (unpublished).

28. Rothenberg, M. S., Physics Today, 29, 17 (Feb 1976).

29. "The free electron laser," Scien. American 236, 62 (Jun 1977).

30. Schwarzchild, B., Physics Today 36, 17 (Dec 1983).

31. Lasers and Applications 2, 40 (Oct 1983).

32. Robinson, A., Science 221, 937 (Sep 1983).

33. Robinson, A., Science 226, 153 (Oct 1984).

34. Schwarzschild, B., Physics Today 37, 19 (Nov 1984).

35. Schwarzschild, B., Physics Today 37, 21 (Nov 1984).

36. Robinson, A., Science 226, 1300 (Dec 1984).

37. Thomsen, D. E., Science News 126, 359 (Dec 1984).

38. Pellegrini, C., IEEE Trans. Nucl. Sci., NS-26, 3791 (1979).

39. Prosnitz, D., "Free Electron Lasers," in CRC Handbook of Laser Science and Technology 1, Weber, M. J., editor, CRC Press, Boca Raton, p. 425 (1982).

40. Morton, P. L., IEEE Trans. Nucl. Sci. NS-28, 3125 (1981).

41. IEEE Journal of Quant. Elec., QE-17, No. 8 (Aug 1981).

42. IEEE Journal of Quant. Elec., QE-19, No. 3 (Mar 1983).

43. Jacobs, S. F., Sargent III, M., Scully, M. O., editors, Novel Sources of Coherent Radiation, Physics of Quant. Elec., 5, Addison-Wesley, Reading, MA (1978).

44. Jacobs, S. F., Pilloff, H. S., Sargent III, M., Scully, M. O., Spitzer, R., editors, Free Electron Generators of Coherent Radiation, Physics of Quant. Elec. 7, Addison-Wesley, Reading, MA (1980).

45. Jacobs, S. F., Pilloff, H. S., Sargent III, M., Scully, M. O., Spitzer, R., editors, Free Electron Generators of Coherent Radiation, Physics of Quant. Elec. 8, Addison-Wesley, Reading, MA (1982).

46. Jacobs, S. F., Pilloff, H. S., Sargent III, M., Scully, M. O., Spitzer, R., editors, Free Electron Generators of Coherent Radiation, Physics of Quant. Elect. 9, Addison-Wesley, Reading, MA (1982).

47. Bendor Free Electron Laser Conference, Journal de Physique, Colloq. C1, supplement au $n^{o}2$, Tome 44 (Feb 1983).

48. Brau, C. A., Jacobs, S. F., Scully, M. O., editors, Free Electron Generators of Coherent Radiation, SPIE 453 (1984).

49. Motz, H., Thon, W., and Whitehurst, R. N., J. Appl. Phys. 24, 826 (1953).

50. Phillips, R. M., IRE Trans. Electron Dev., 17, 231 (1960).

51. Schawlow, A. L. and Townes, C. H., Phys. Rev. 112, 1940 (1958); Maiman, T. H., Phys. Rev. Lett. 4, 564 (1960).

52. Palmer, R. B., J. Appl. Phys. 43, 3014 (1972); Csonka, P. Particle Accelerators 8, 225 (1978); Robinson, K., unpublished notes.

53. Hopf, F. A. Meystre, P., Scully, M. O., Louisell, W. H., Phys. Rev. Lett. 37, 1342 (1976).

54. Colson, W. B., Phys. Lett., 64A, 190 (1977); Colson, W. B. and Ride, S. K., Phys. Lett. 76A, 379 (1980).

55. Madey, J. M. J., Nuovo Cimento B50, 64 (1979).

56. Kroll, N. M., Morton, P. L. and Rosenbluth, M. N., IEEE J. Quant. Elec. QE-27, 1436-68 (1981).

57. Vinokurov, N. A. and Shrinsky, A. N., Institute of Nuclear Physics, Novosibirsk, Report No. INP 77-59, (unpublished) (1977).

58. Luccio, A. and Krinsky, S., see Ref. 45, p. 181 (1982).

59. Dattoli, G. and Renieri, A., "Experimental and theoretical aspects of the free electron laser," Laser Handbook 4, Stitch, M. L. and Bass, M. S., editors, North Holland, Amsterdam (to be published).

60. Scharlemann, E. T., Lawrence Livermore National Laboratory ELF Note 105P, (published) (1984).

61. Kroll, N. and Rosenbluth, M., see Ref. 44, p. 147.

62. Fawley, W. M., Prosnitz, D., Scharlemann, E. T., submitted to Phys. Rev. A (1985), Lawrence Livermore National Laboratory Rpt UCRL-90838 (unpublished) (1984).

63. Scharlemann, E. T., Sessler, A. M. and Wurtele, J. S., submitted to the Proc. of the Como Conf.; Lawrence Livermore National Laboratory Rpt UCRL-91476, (unpublished) (1984).

64. Scharlemann, E. T., Sessler, A. M. and Wurtele, J. S., submitted to Phys. Rev. Lett. (1984).

65. Moore, G. T., Optics Communicat. 52, 46 (1984); Moore, G. T., submitted to the Proc. of the Como Conf., IMO Rpt 84-14 (unpublished) (1984).

66. Colson, W. B. and Elleaume, P., Appl. Phys., B29, 1-9 (1982).

67. Colson, W. B. and Renieri, A., see Ref. 47, Colloque C1-11.

68. Al-Abawi, H., Hopf, F. A., Moore, G. T. and Scully, M. O., Opt. Commun., 30, 235 (1979).

69. Eckstein, J. N., et al, Physics of Quant. Elec., 8, 49, Addison-Wesley, (1982).

70. Benson, S., Deacon, et al, Phys. Rev. Lett., 48, 235 (1982).

71. Kroll, N. M. and Rosenbluth, M. N., see Ref. 44, p. 147.

72. Colson, W. B., IEEE J. Quant. Elec., QE-17, 1417-27 (1981).

73. Fessenden, T. J., et al, Proc. of the 4th Int'l Conf. on High Power Electron and Ion Beam Research and Technology, p. 813 (1981).

74. Briggs, R. J., et al, IEEE Trans. on Nucl. Sci., NS-28, 3360 (1981), Doucet, H. J. and Brezzi, J. M., editors, Palaiseau.

75. Takeda, S., Workshop on the Generation of High Fields, Frascati, Sep 25-Oct 1, 1984.

76. Warren, R. M., et al, Lasers 84 Technical Digest, p. 20 (1984).

77. Elias, L., Lasers 84 Technical Digest, p. 25 (1984).

78. Boehmer, H., et al, Phys. Rev. Lett., 48, 141 (1982).

79. Birx, D. L., et al, "A Multipurpose 5 MeV Linear Induction Accelerator," Proc. of the IEEE Power Modulator Symposium, June 1984, Lawrence Livermore National Laboratory Rpt UCRL-90554 (unpublished) (1984).

80. Shaw, E. D., Chichester, R. J. and Sprenger, W. C., "Lasers 84," Technical Digest, p. 19 (1984).

81. Smith, S. D., et al, see Ref. 45, p. 275.

82. Bizzarri, U., et al, Lasers 84 Technical Digest, p. 21 (1984).

83. Leiss, J., Norris, N. J., Wilson, M. A., Part. Accel. 10, 223 (1980).

84. Billardon, M., et al, see Ref. 15, p. 1652.

85. Deacon, D. A. G., Lasers 84 Technical Digest, p. 27 (1984).

86. Ballili, J. P. et al "Report of Prospectives for Super ACO," LURE, Orsay, Internal Report (unpublished) (April 1981).

87. Peterson, J. M., et al, contributed paper to the Castelgandolfo Conf, Nucl. Inst. and Methods in Physics Research, to be published (1985).

88. Orzechowski, T. J., et al, see Ref. 48, p. 65.

89. Billardon, M., et al, see Ref. 47, p. C1-29.

90. Elleaume, P., J. Physique 45, 997 (1984).

91. Renieri, A., Nuovo Cimento B59, 64 (1979).

92. Freund, H. P., see Ref. 48, p. 361.

93. Lin, A. T., see Ref. 48, p. 336.

94. Tsumoru, S., et al, Jap. Journal of Appl. Phys. 22, 844 (1983).

95. Granatstein, V. L., Carmel, Y. and Gover, A., see Ref. 48, p. 344.

96. Elias, L. B., Phys. Rev. Lett. 42, 977, (1980).

97. Freund, H. P., and Ganguly, A. K., see Ref. 48, p. 367.

98. Piestrup, M. A. and Finman, P. F., see Ref. 48, p. 384.

99. Fauchet, A. M., et al, see Ref. 48, p. 423.

100. Deacon, D. A. G., Phys. Rev. Lett. 44, 449 (1980).

101. Deacon, D. A. G., Physics Report 76, 349 (1981).

102. Gaupp, A., see Ref. 47, p. C1-147.

103. Madey, J. M. J. and Pellegrini, C., editors, AIP Conf Proc, Brookhaven, Sep 1983, 118, New York (1984).

104. Proc of the Conf. on Coherent and Collective Properties in the Interaction of Relativistic Electrons and Electromagnetic Radiation, Como, Sep 1984, Nuclear Instruments and Methods in Physics Research, (to be published).

Figure Legends

Figure 1 The basic elements of a free electron laser (FEL) oscillator are a high-quality relativistic electron beam, an undulator magnet which causes the electrons to wiggle, and the resonant optical cavity to provide feedback.

Figure 2 A practical design for constructing the undulator field is shown at the top where eight permanent magnets are used to form one undulator period. The interaction of an initially azimuthally uniform electron beam, with the radiation in an FEL causes the electron beam to bunch in an optical wavelength. It is this bunching which causes coherent radiation.

Figure 3 Free electron lasers can be in a variety of configurations which are depicted here. In fact, three of these five types have already operated.

Figure 4 FELs grew out of the development of electron tubes and atomic lasers. They retain some of the good qualities of both.

Figure 5 The electron phase space follows sample electrons through the undulator. The separatrix is shown as a guide to the phase space paths. The electron fluid grows darker as it passes through the undulator. (The same representation is employed in Figures 6 and 8.) Bunching at the phase π leads to gain, but also affects the optical phase.

Figure 6 In the high gain case, there is a substantial optical phase change shift which shifts the separatrix. The height of the separatrix is proportional to the $|a|^{1/2}$ and grows with the high gain.

Figure 7 The final gain and phase of the optical wave are plotted as a function of ν_0. Experimental points are superimposed to show agreement between small amplitude theory and experiment [Orsay] (89).

Figure 8 Phase space evolution in the strong field regime. The "synchrotron" motion of the particles has led to saturation and energy is no longer transferred from the electrons to the optical wave. Even in saturation the phase of the optical wave evolves.

Figure 9 In a tapered FEL some electrons are trapped near the phase which drives the optical wave. The untrapped electrons are distributed over many phases and do not drive the wave.

Figure 10 Typically FELs are made to produce the fundamental mode in an optical resonator which has a Gaussian shape in x and y. A higher order mode is excited here by moving the electron beam off of the resonator axis. The theoretical calculation employed the parameters of the original Stanford FEL.(11)

Figure 11 Intense electron beams going through an FEL can provide optical guiding of the radiation. In the absence of guiding the radiation would diffract out of the electron beam long before the end of the undulator.

Figure 12 The growth of coherence in the optical wave is shown by following 100 modes from spontaneous emission. The photon density at the wavelengths near peak gain grow more rapidly than surrounding wavelengths. This narrows the spectrum after only 100 passes. Evidently the laser can become narrow-band.

Figure 13 When the electron synchrotron oscillations mix with the carrier wave, sidebands can be formed. Over many passes the optical wave develops a modulation whose period matches the synchrotron period. The optical power increases with the addition energy of the sideband.

Table 1 Operation of free electron lasers

Name	Year of 1st Operation	Wavelength	Peak Power	Type*
Stanford (11)	1976, 1977	10 μm, 3.4μm	130 kW	A,O
Columbia (25)	1977	1.5 mm	8 MW	ASE
NRL (26)	1977	400 μm	1 MW	ASE
NRL/Columbia (23)	1978	400 μm	1 MW	ASE,O
LANL (13)	1981, 1982	10.6 μm	10 MW	A,O
NRL (12)	1981 1983	4.6 mm - 3.1 mm 35 GHz	75 MW 17 MW	ASE A
Orsay (15)	1981, 1983	6500 Å	60 MW	A,O
MSNW (14)	1982	10.6 μm	(1)	A
Frascati (22)	1983	5145 Å	(2)	A,O
TRW (16)	1983	1.57 μm	1.2 MW	O
NRL (17)	1984	1 cm	20 MW	ASE
MIT (19)	1984	4.3 cm - 1.7 cm	100 kW	A
UCSB (20)	1984	0.4 mm	8 kW	O
LLNL (18)	1984	8.6 mm	80 MW	A
Hughes (21)	1984	1 cm	60 kW	O
Erevan (24)	1984	20-40 μm	10 W	O
Novosibirsk (27)	1984	6000 A°	(3)	A,O

* A - Amplifier
O - Oscillator
ASE - Amplified Spontaneous Emission
(1) - Output power not measured, but peak loss of electron energy was observed to be 9%
(2) - With an input laser power of 6W, a gain of 3×10^{-4} was measured.
(3) - A gain of 1.5% was measured.

Table 2 Selected FEL accelerators

Accelerator	Beam energy (MeV)	Peak beam current (A)	Pulse length	Pulse rep rate (Hz)	Beam brightness $\left(\frac{A}{cm^2 rad^2}\right)$		$\frac{\Delta\gamma}{\gamma}$
ETA (73) I	5	1000	15 ns	1.0	2×10^4 (at 2.5 MeV)	(1)	(3)
ATA (74) I	50	1000–10,000	50 ns	1.0	$5\text{–}6\times10^4$ (at 4 MeV)	(1)	(3)
Osaka (75) RF	20–38	1000–3000	16 ps	1.0–720	$1.8\text{–}5.4\times10^7$		7×10^{-3}
LANL (76) RF	20	35–65	40 ps(micro) 100 μs (macro)	1.0	7.0×10^5		2×10^{-2}
UC Santa Barbara (77) DC	2.5	1.25	30 μs-dc	-	3.8×10^6	(1)	(3)
Stanford SCA (78) RF	80–120	4	2 ps (micro) 10 ms (macro)	10	8×10^6	(2)	10^{-4}
LLNL High Brightness Test Stand (79) I	2	20–900	70 ns	1	1.5×10^5		(3)
Bell Labs Microtron (80)	10–20	1–5	10 ps (micro) 10 μs (macro)	100	4.2×10^2	(4)	-
UK RF Linac (81) RF	30–100	10.0	60 ps (micro) 8.5 μs (macro)	100	2.5×10^4		10^{-2}
Frascati ENEA Microtron (82)	20	6.5	23 ps (micro) 12 μs (macro)	10	4.5×10^4		1.2×10^{-3}
NRL Induction (83) I	0.55–0.75	200	2 μs	single shot	6.4×10^3		3×10^{-2}
MIT Pulsed Device (19)	2.0	1100	20 ns	0.01	1.4×10^6		< .01
Orsay ACO (84) SR	163	3.3	0.5 - 1 ns	27 MHz	3.8×10^6	(2)	10^{-3}
Stanford SXRC Ring Development (85) SR	1.2 GeV	270	33 ps	20 MHz	4×10^8	(2)	6×10^{-4}
Orsay Super ACO Development (86) SR	400	50	25 ps–300 ps	4.8 MHz	1.7×10^8	(2)	3×10^{-4}
LBL Design (87) SR	750	327	41 ps	2 MHz	2.8×10^9	(2)	2×10^{-3}

(1) Edge emittance
(2) 1/e in x and 1/e in x' emittance, or approximately 9 times edge brightness
(3) $\Delta\gamma/\gamma$ unmeasurably small; variation of γ during a pulse
(4) Estimated

I Induction linac
RF RF linac
SR Storage ring
DC DC accelerator

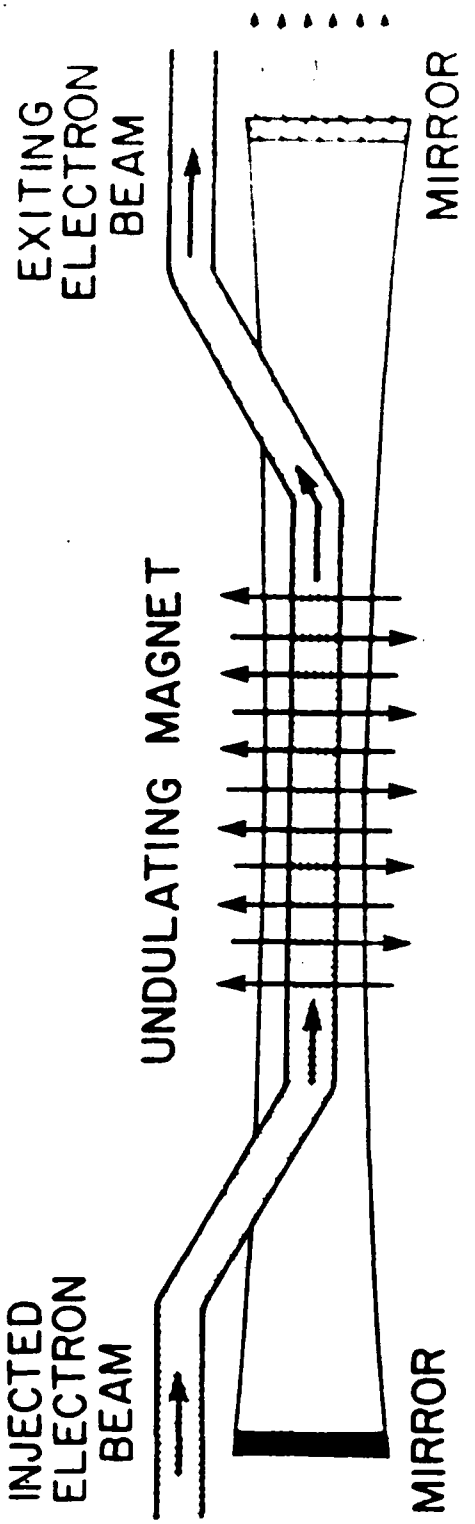
EXITING
ELECTRON
BEAM
MIRROR
UNDULATING MAGNET
OPTICAL RESONATOR
INJECTED
ELECTRON
BEAM
MIRROR

Figure 1

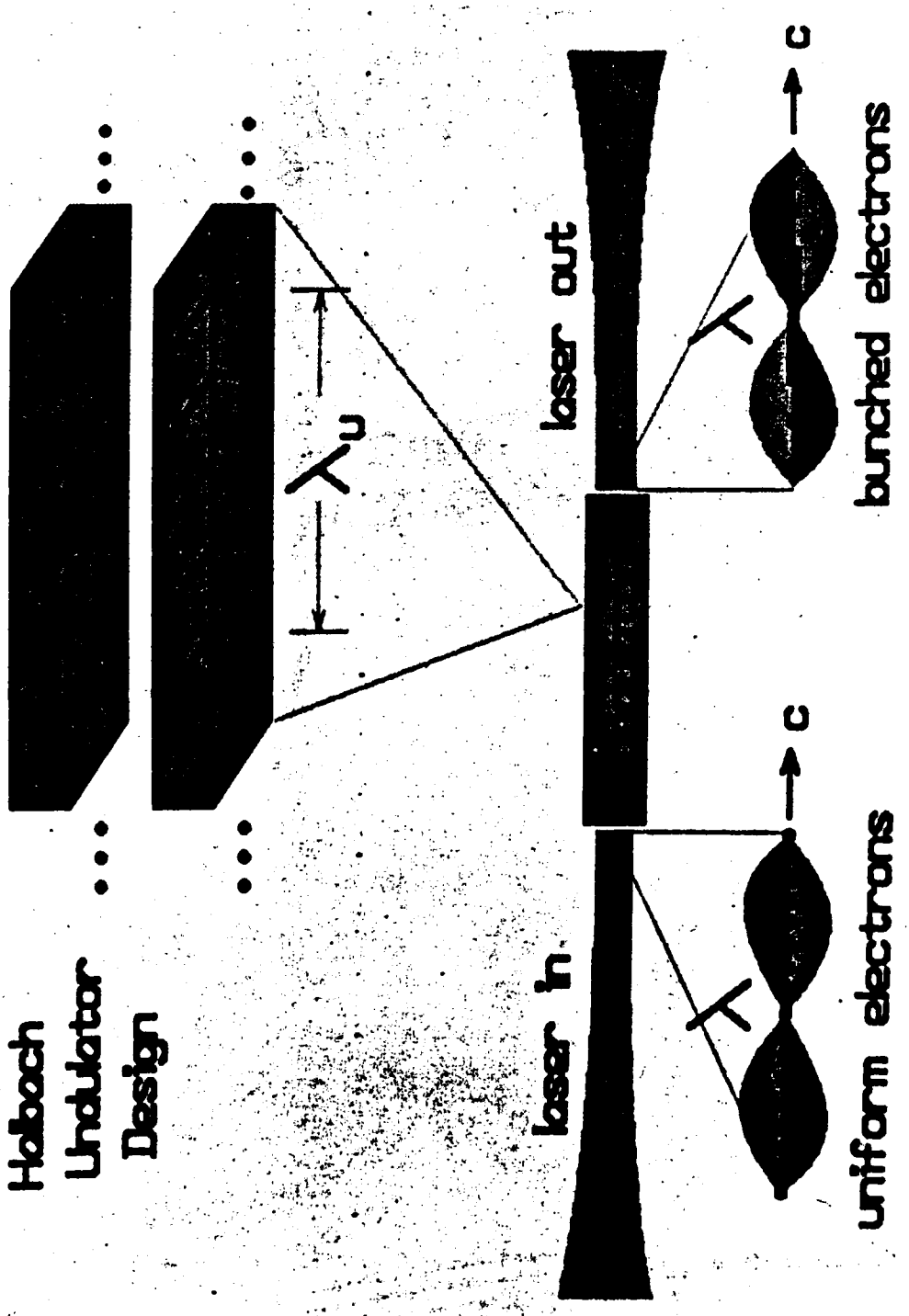
Halbach
Undulator
Design
λ_u
laser out
laser in
c
bunched electrons
uniform electrons

Figure 2

Some FEL Configurations

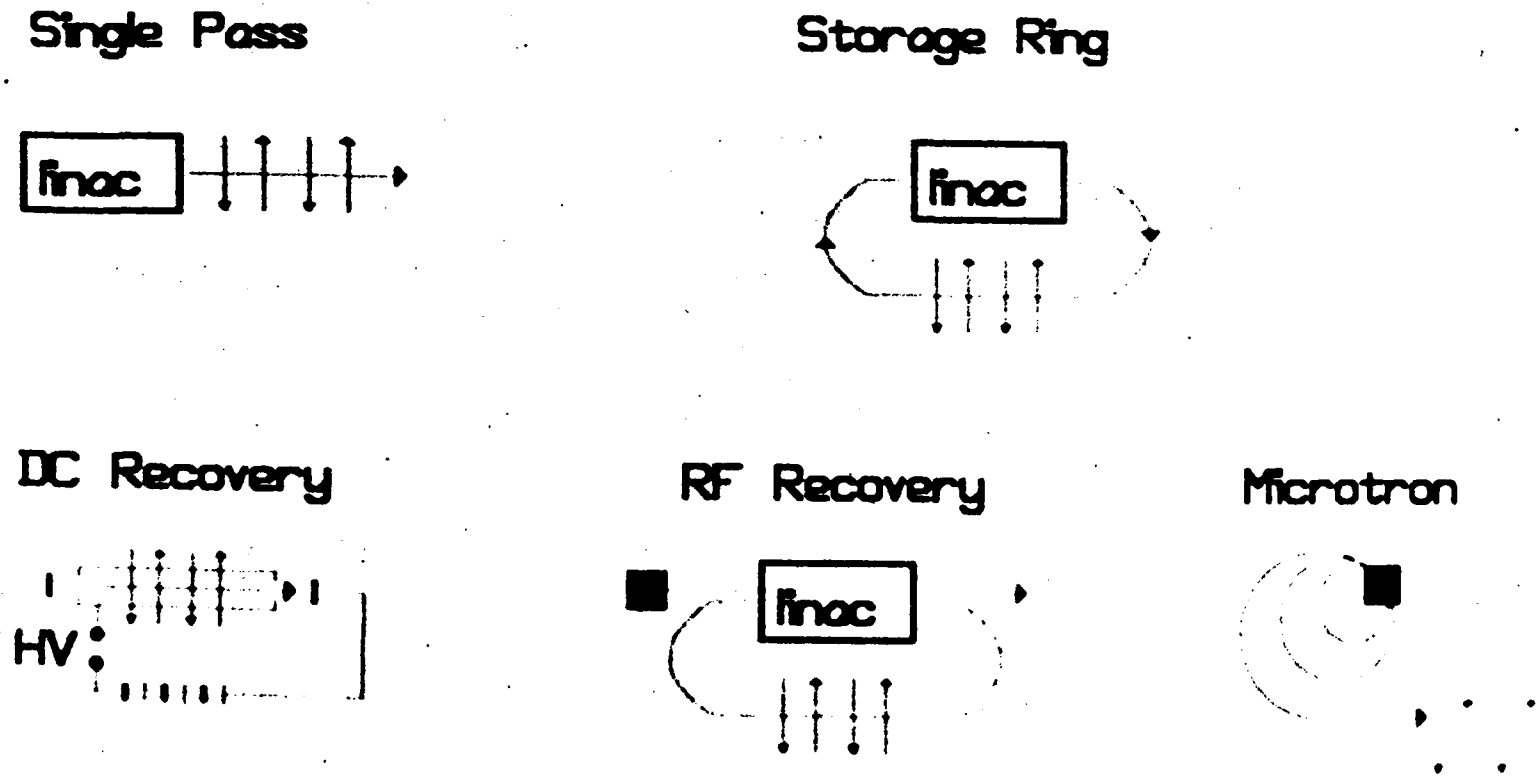

Figure 3

GENERAL HISTORY

- Electron Tubes (1930's -> 1960's)
  - free non-relativistic electrons
  - microwave cavity
    long wavelengths, tunable, efficient

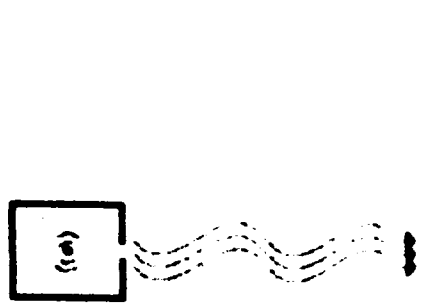

- Atomic & Molecular Lasers (1960's -> now)
  - bound electrons
  - optical resonator
    short wavelengths

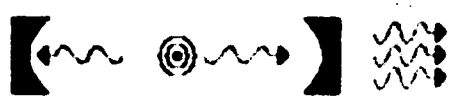

- Free-Electron Lasers (1976 -> now)
  - free relativistic electrons
  - optical resonator
    short wavelengths, tunable, efficient

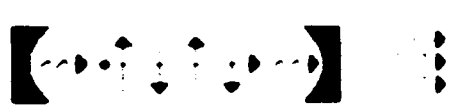

Figure 4

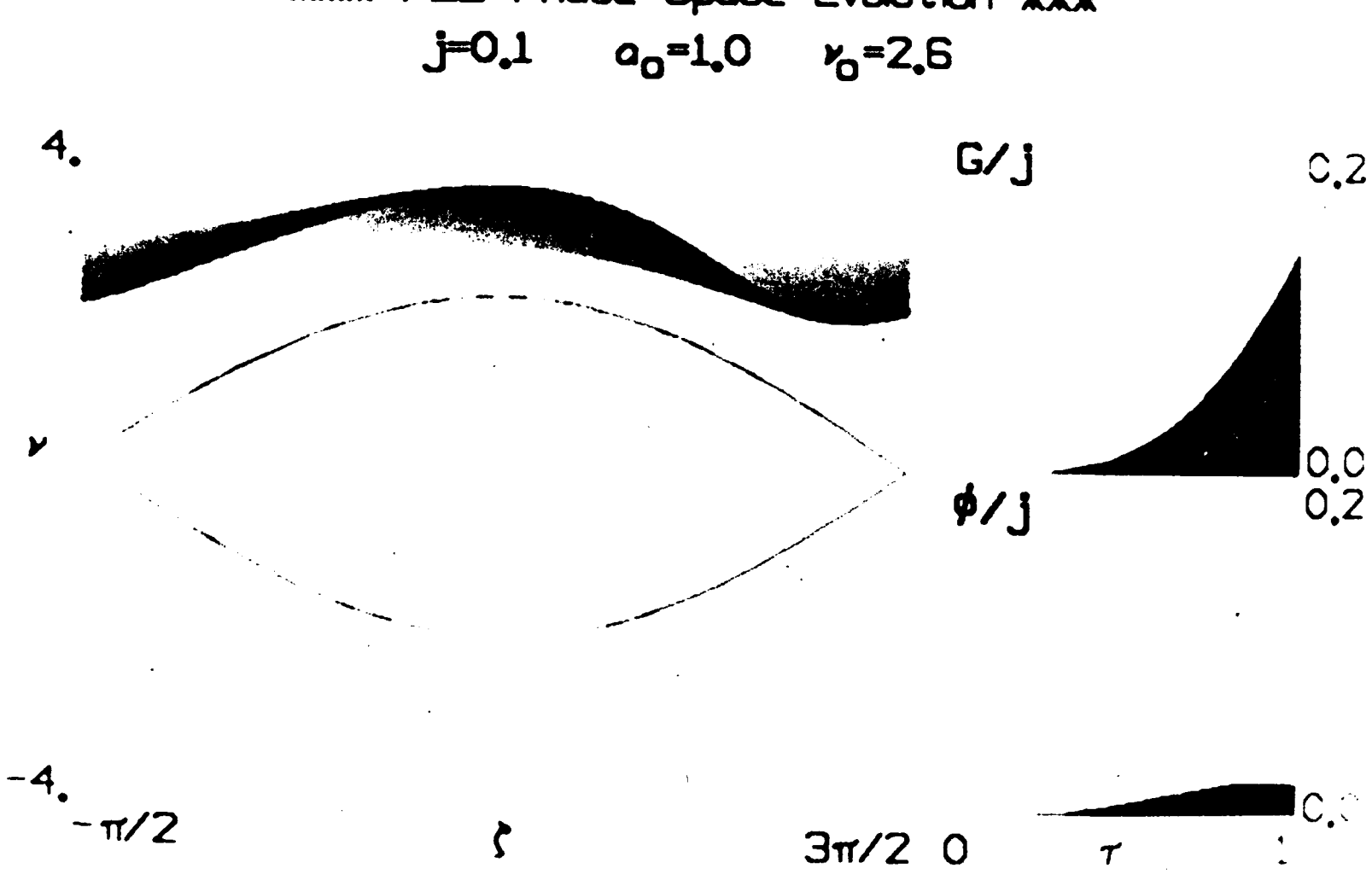
*** FEL Phase Space Evolution ***
j=0.1 a_0=1.0 ν_0=2.6
4.
G/j
0.2
ν
0.0
ϕ/j
0.2
-4.
-π/2
ζ
3π/2 0
τ
1

Figure 5

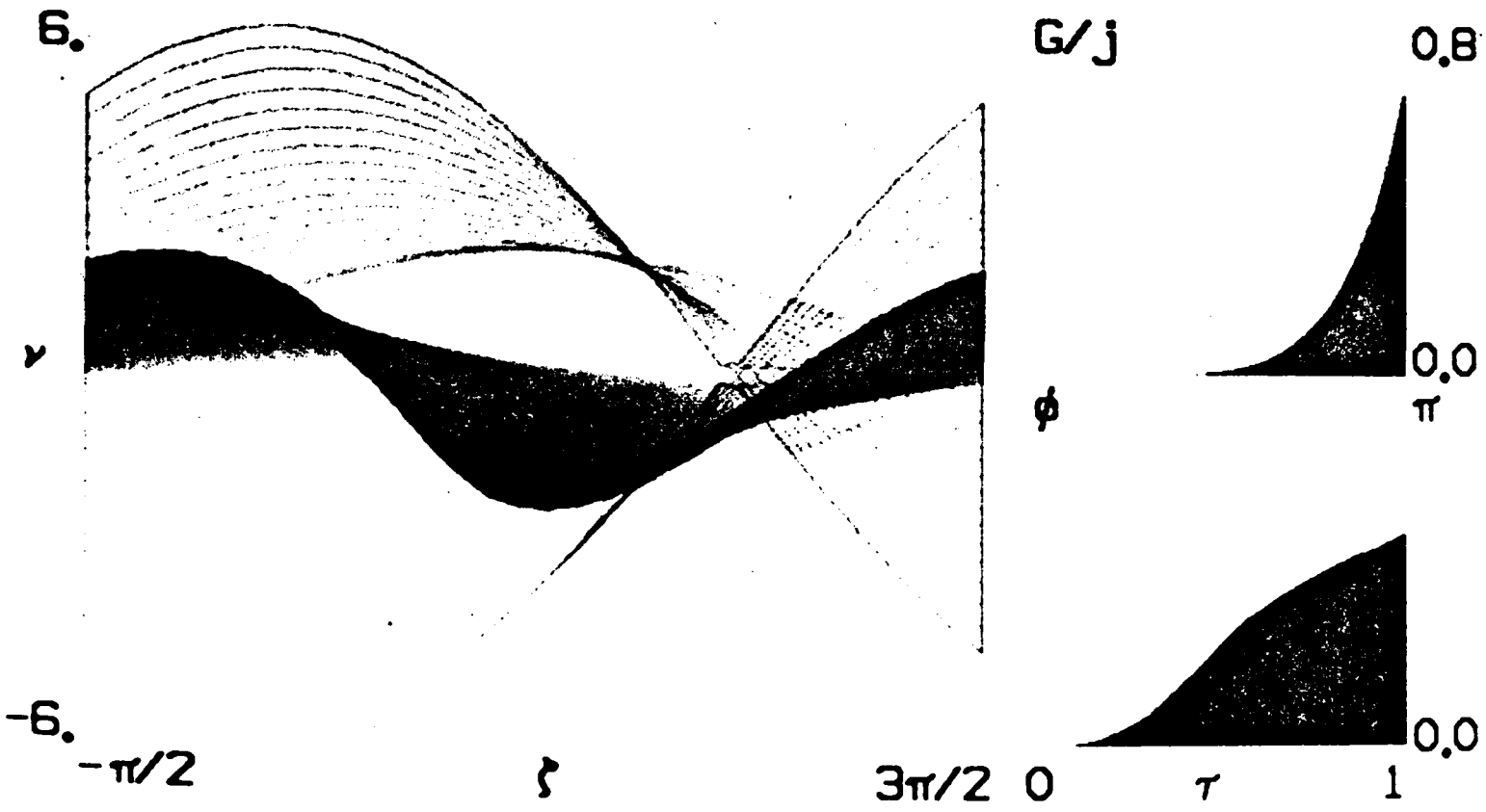
*** FEL Phase Space Evolution ***
j=100. a_0=1.0 ν_0=0.0
6.
ν
-6.
-π/2
ζ
3π/2
G/j
0.8
0.0
φ
π
0
τ
1
0.0

Figure 6

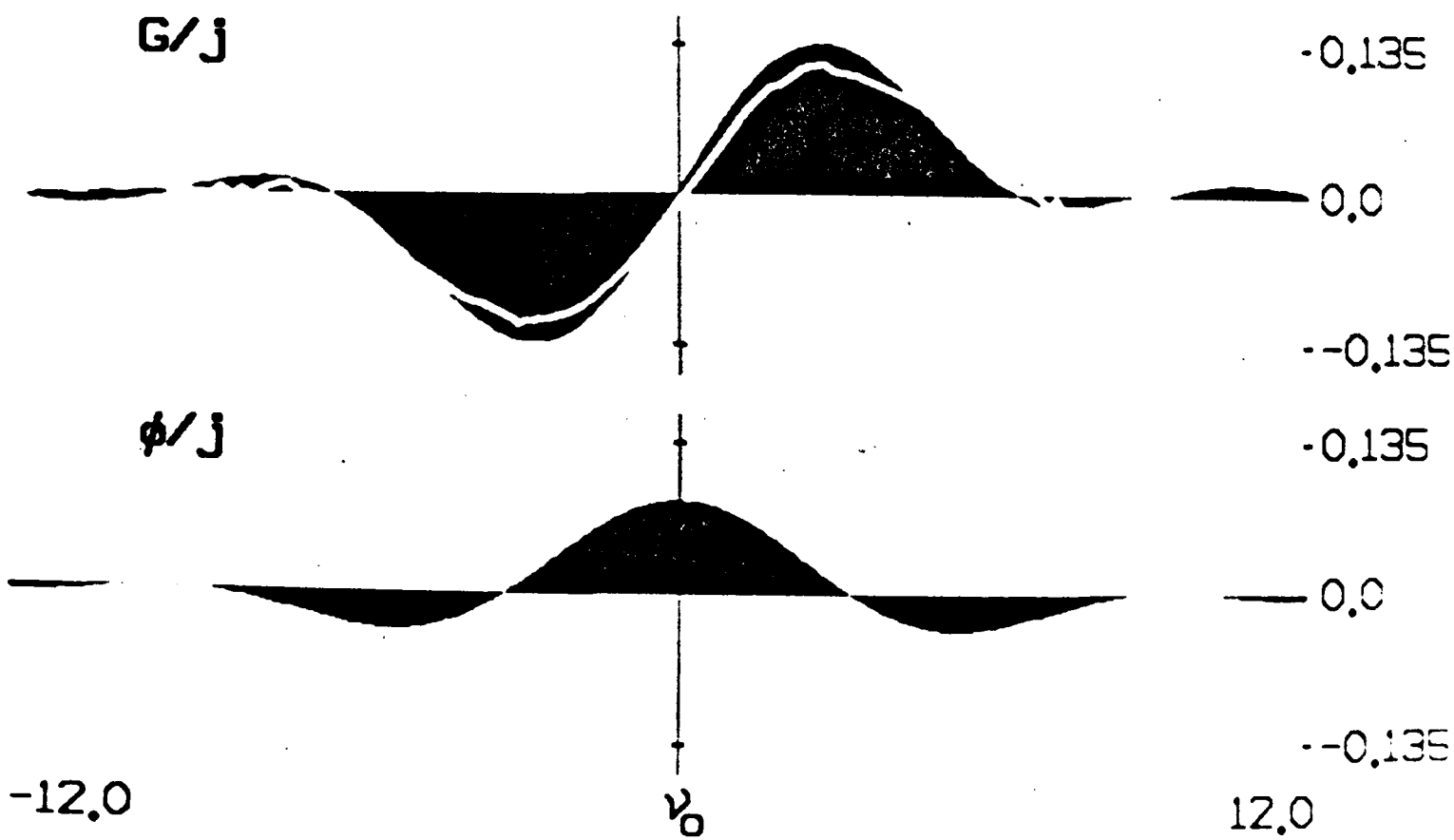
**** Gain and Phase Spectrum ****
j=0.1 a_0=0.1
G/j
-0.135
0.0
--0.135
ϕ/j
-0.135
0.0
--0.135
-12.0
ν_0
12.0

Figure 7

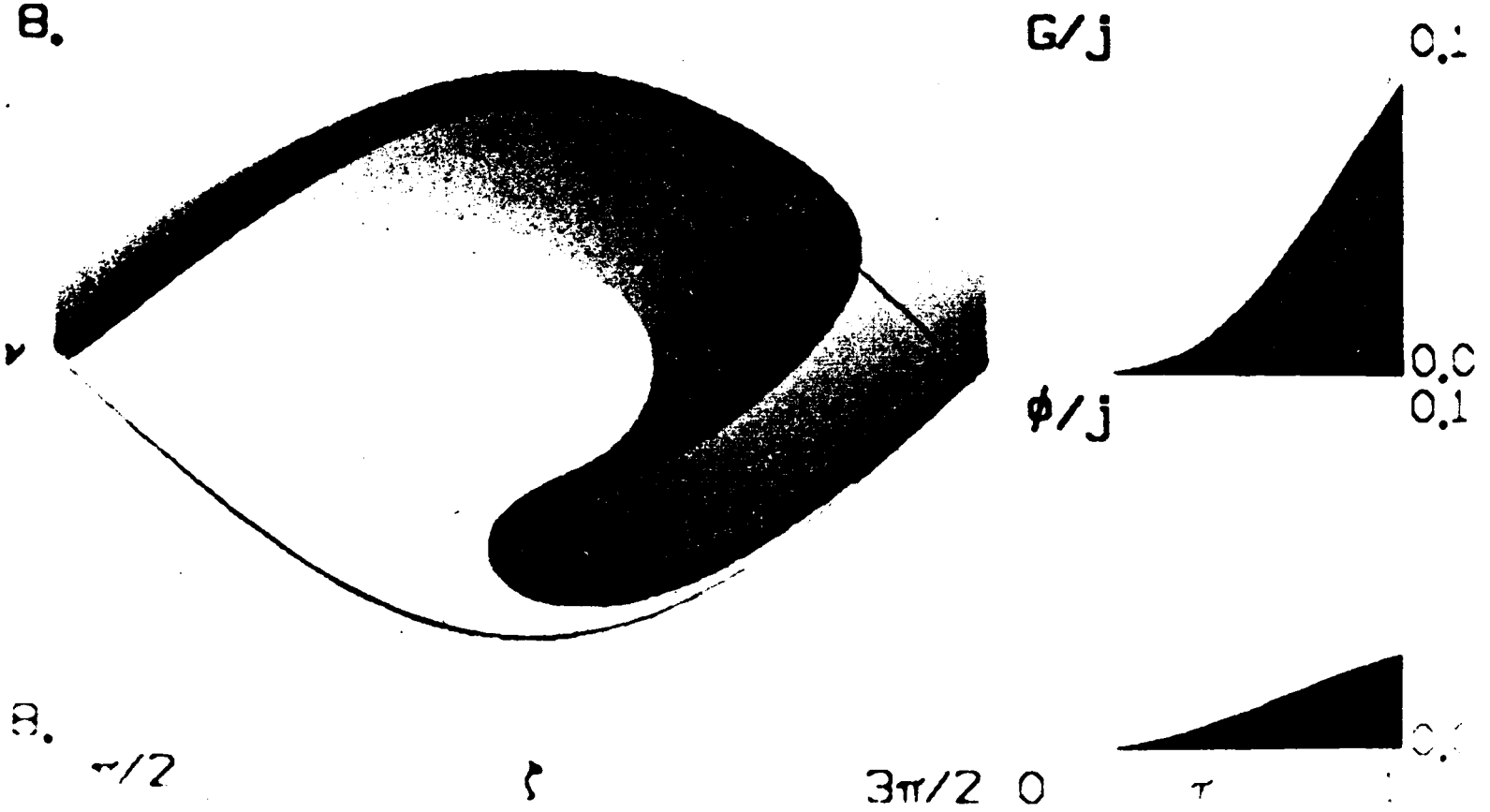
*** FEL Phase Space Evolution ***
j=1. a_0=8.0 ν_0=2.6
8.
G/j
0.1
0.0
0.1
ϕ/j
3.
-/2
3π/2 0

Figure 8

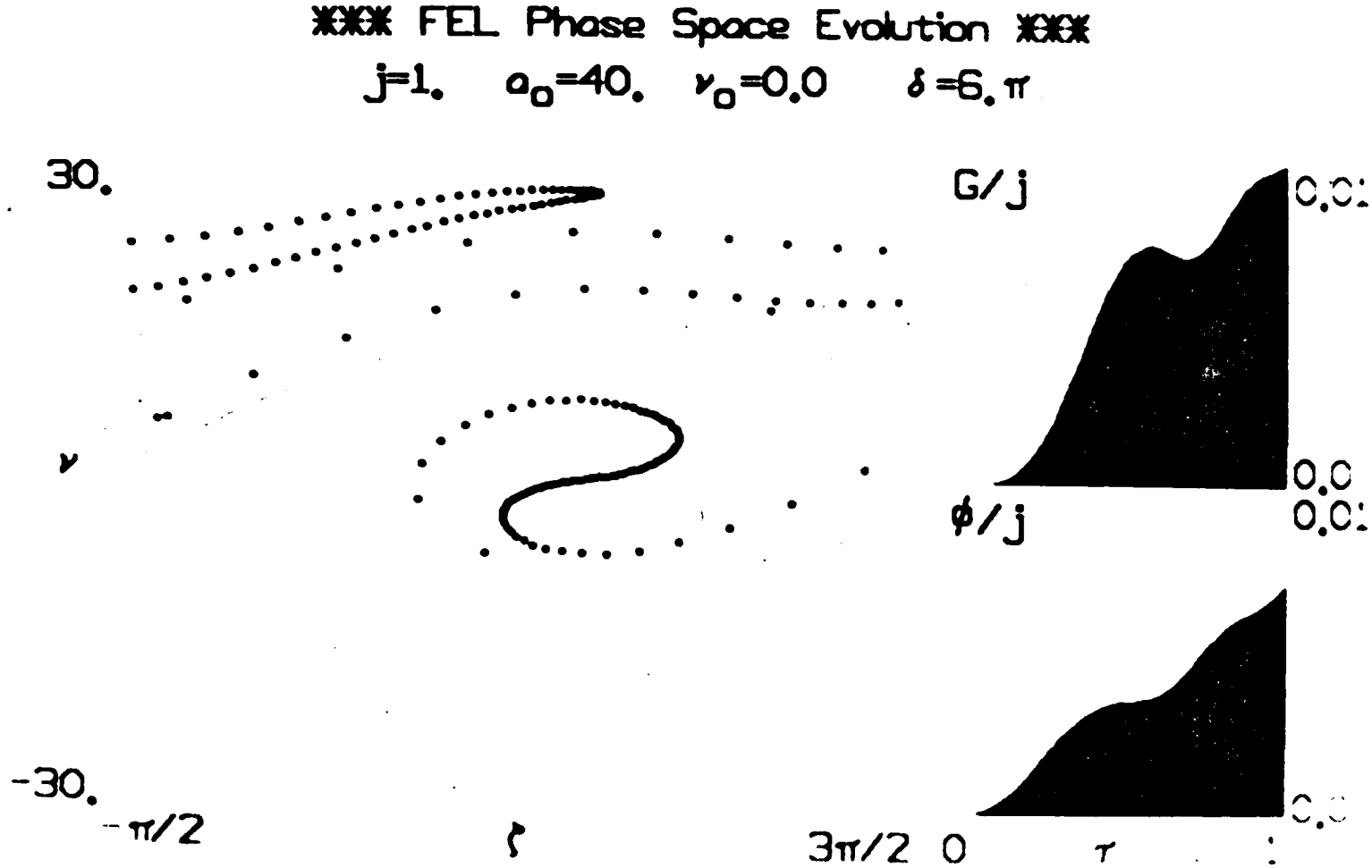
*** FEL Phase Space Evolution ***
j=1. a_0=40. ν_0=0.0 δ=6.π
30.
-30.
ν
ζ
-π/2
3π/2
0
τ
G/j
ϕ/j
0.0

Figure 9

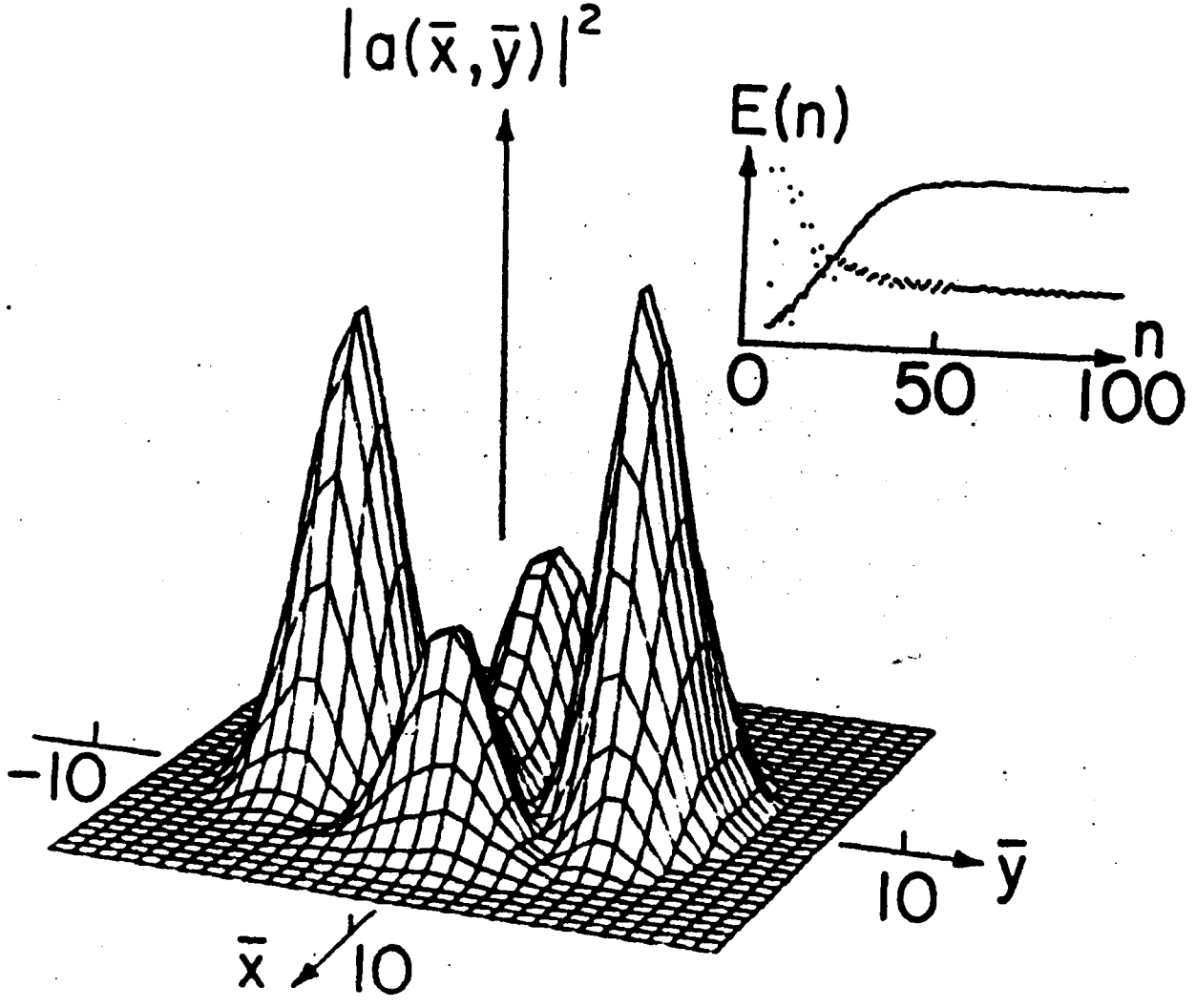

Figure 10

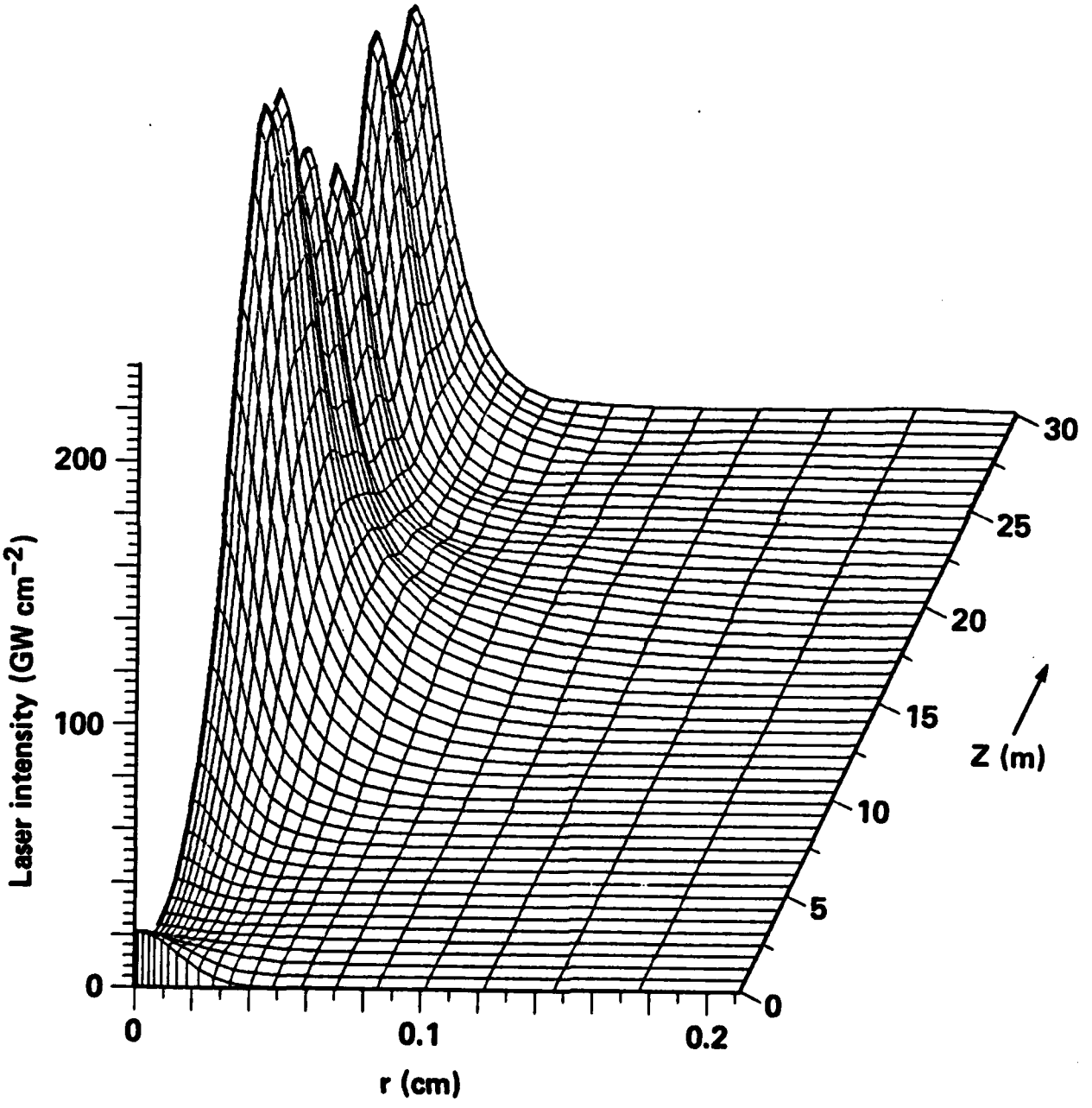

Figure 11

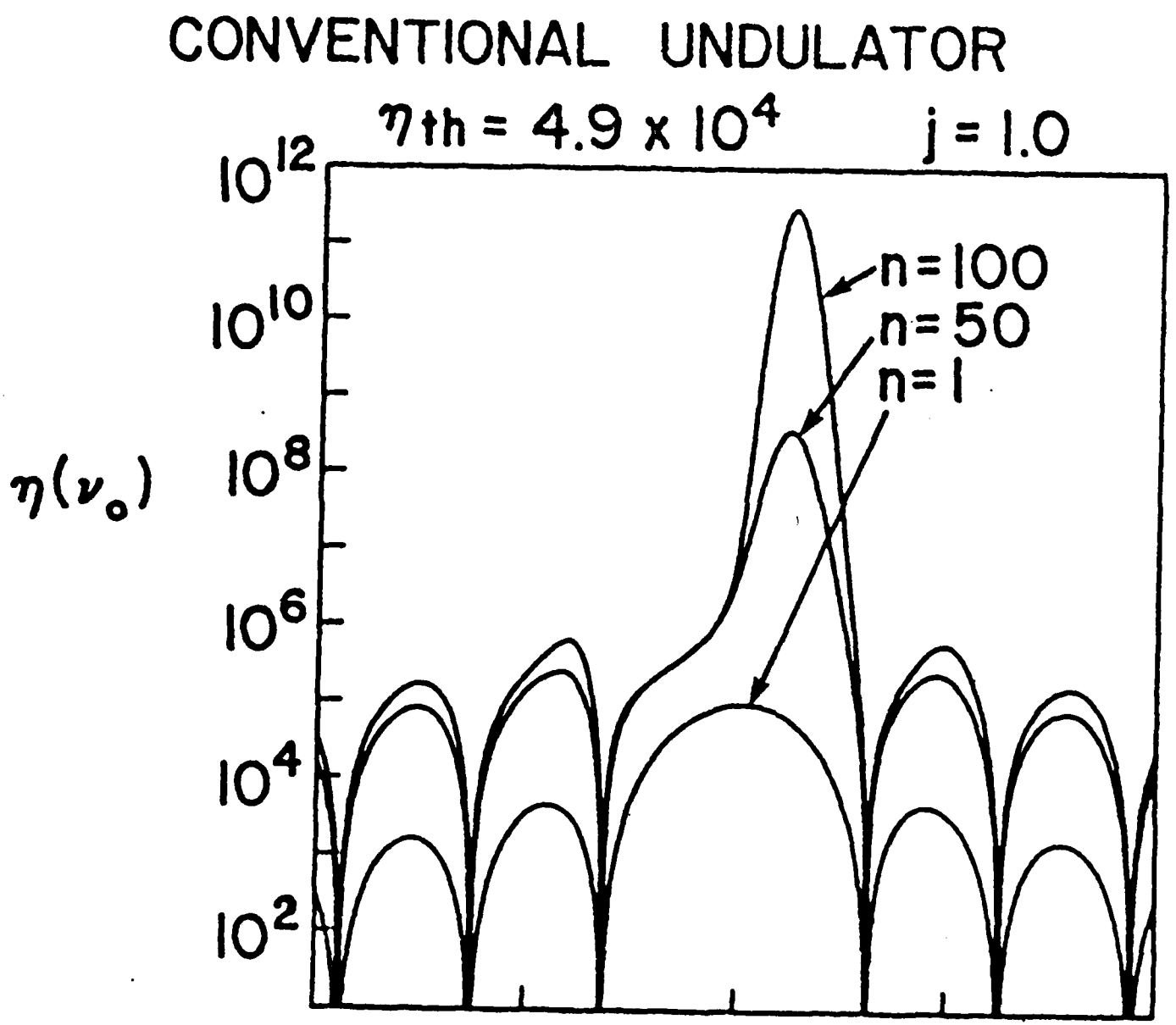
CONVENTIONAL UNDULATOR
ηth = 4.9 x 10^4
j = 1.0
10^12
10^10
10^8
10^6
10^4
10^2
η(ν_o)
n=100
n=50
n=1

Figure 12

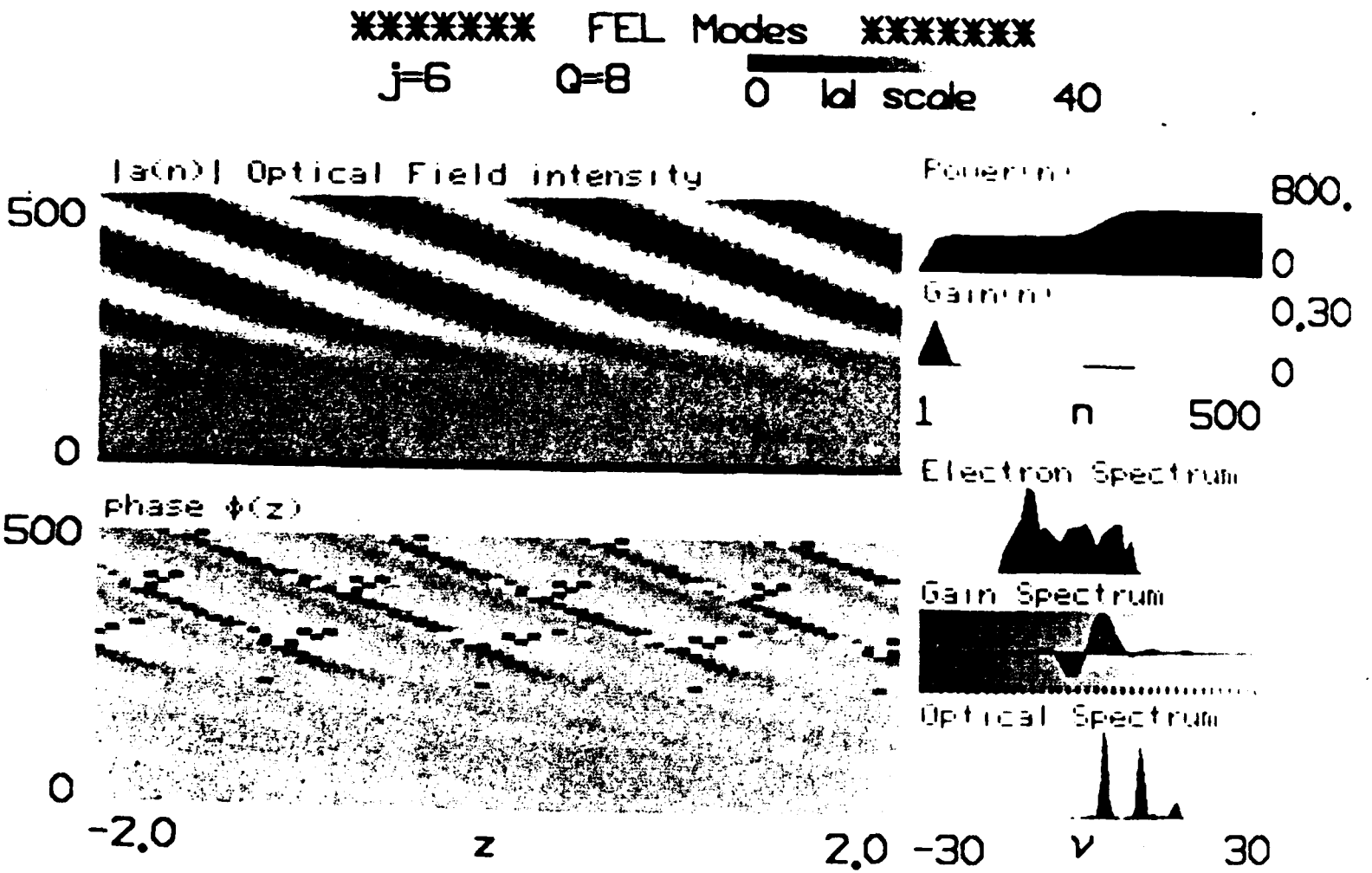
******* FEL Modes *******
j=6 Q=8
0 log scale 40
|a(n)| Optical Field intensity
500
0
Power(n)
800.
0
Gain(n)
0.30
0
1 n 500
Electron Spectrum
Gain Spectrum
Optical Spectrum
phase ϕ(z)
500
0
-2.0 z 2.0
-30 ν 30

Figure 13

END

FILMED

10-85

DTIC